CHAPTER IV
RESULTS AND DISCUSSION

4.1 Dynamic mechanical analysis

The dynamic mechanical properties such as storage modulus (G'), loss modulus (G") and damping (tanδ) of pure components and their blends were evaluated from –100 to 40°C at frequency of 1 rad/sec and 0.06% strain. Figure 4.1-4.3 show the variation of tanδ, G' and G" versus temperature for the homopolymers. The tanδ curve of natural rubber shows a peak at –60°C due to the α-transition arising from the segmental motion. This corresponds to the glass transition temperature (T_g) of natural rubber. Linear low-density polyethylene shows the glass transition temperature at –30°C, as shown by maximum point of tanδ peak at -30°C in tanδ vs. temperature curve. Natural

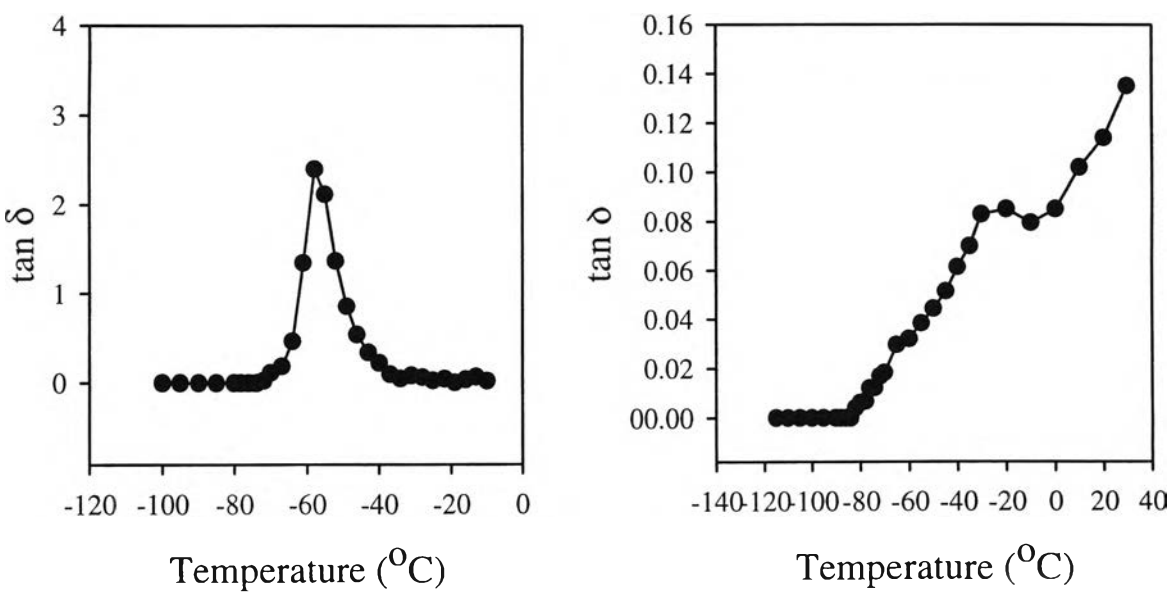

Figure 4.1 Effect of temperature on damping (tanδ) of pure natural rubber and pure linear low-density polyethylene.

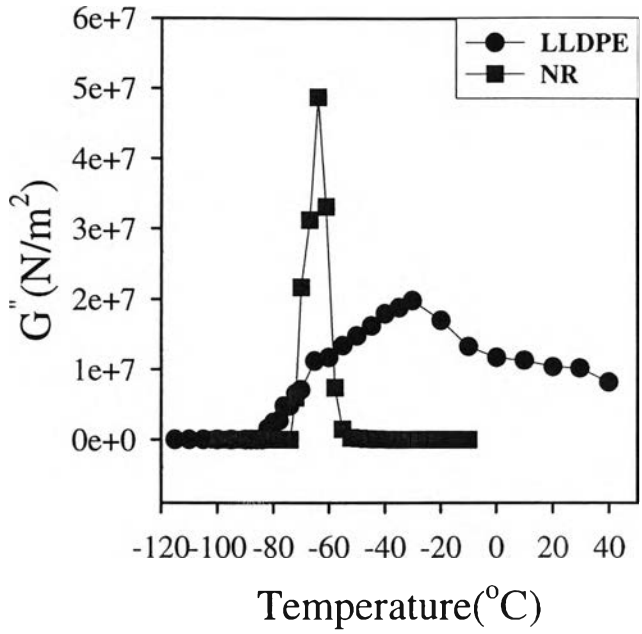

Figure 4.2 Effect of temperature on loss modulus (G") of pure natural rubber and pure linear low-density polyethylene.

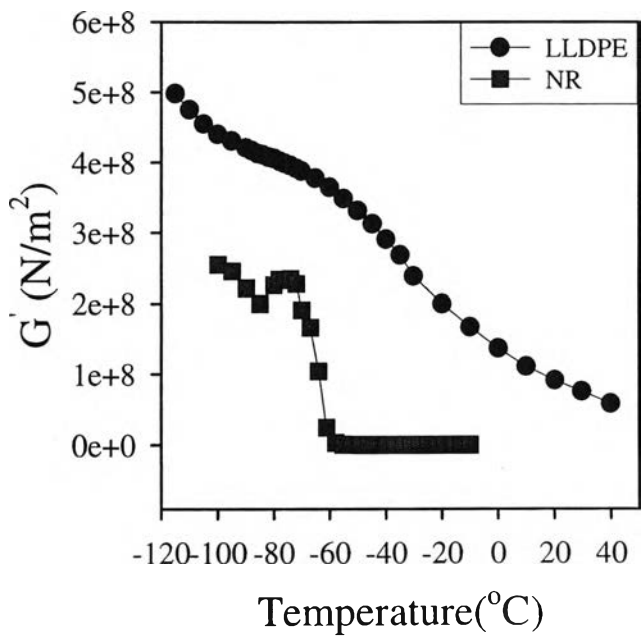

Figure 4.3 Effect of temperature on storage modulus (G') of pure natural rubber and pure linear low-density polyethylene.

rubber has higher damping than linear low-density polyethylene because of its rubbery nature. The loss modulus (G") curve also shows the presence of loss maximum for NR and LLDPE at -60 and -30°C, respectively (Figure 4.2). A. Akhtar *et al.* (1989) have been studied the blends of natural rubber with polyethylene. Their dynamic mechanical properties were examined by using a Rheovibron DDV III C. They found that tanδ peak strongly depends on the content of NR in the HDPE blend. The blend at composition 70/30 HDPE/NR shows a maximum tanδ at-55°C, which corresponds to the glass transition temperature of NR alone, while the glass transition temperature of HDPE lies outside the studied temperature range. N. Roy Choudhury *et al.* (1989) also investigated the dynamic mechanical properties of natural rubber-polyethylene blends by using a dynamic mechanical analyser (Rheovibron DDV III EP). They found that pure PE exhibits transition at –131 and –10°C, respectively while for pure NR, the glass transition is detected at –53°C. In Figure 4.3, the storage modulus of natural rubber shows a drastic fall around T_g, while for linear low-density polyethylene, because of its crystalline nature, the modulus drop is at a slower rate. In crystalline materials, during transition, only the amorphous part undergoes segmental motion, while the crystalline region remains as solid until its temperature of melting (T_m). Hence, in the case of linear low-density polyethylene, which is a crystalline material, the storage modulus drops only in a lesser extent than that in NR as a result of the relaxation process.

Dynamic mechanical studies were used to predict the miscibility of the system by various researchers. Generally, for an incompatible blend, the tanδ vs. temperature curve shows the presence of two tanδ or damping peaks corresponding to the glass transition temperatures of individual components (Thomas and George, 1992). For the compatible blend the curve shows only a single peak. The variation of tanδ with temperature for the 70/30 LLDPE/NR blend is shown in Figure 4.4. The blends show two tanδ peaks around –64

and –45°C, which correspond to the glass transition temperatures of natural rubber and linear low-density polyethylene respectively. Two separate peaks corresponding to the T_g's of NR and LLDPE indicate that the blends are not compatible. The T_g corresponding to LLDPE is shifted to a lower temperature upon the addition of NR. This may be due to the plasticizing effect of NR, by which the chain mobility of LLDPE is increased.

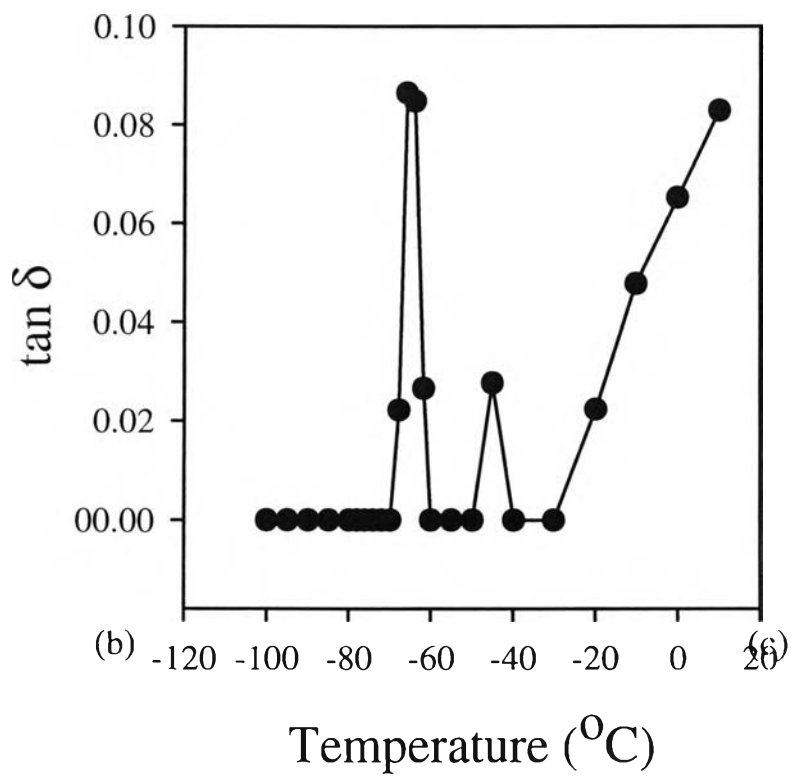

Figure 4.4 Effect of temperature on damping (tanδ) of 70/30 LLDPE/NR blend without maleic anhydride.

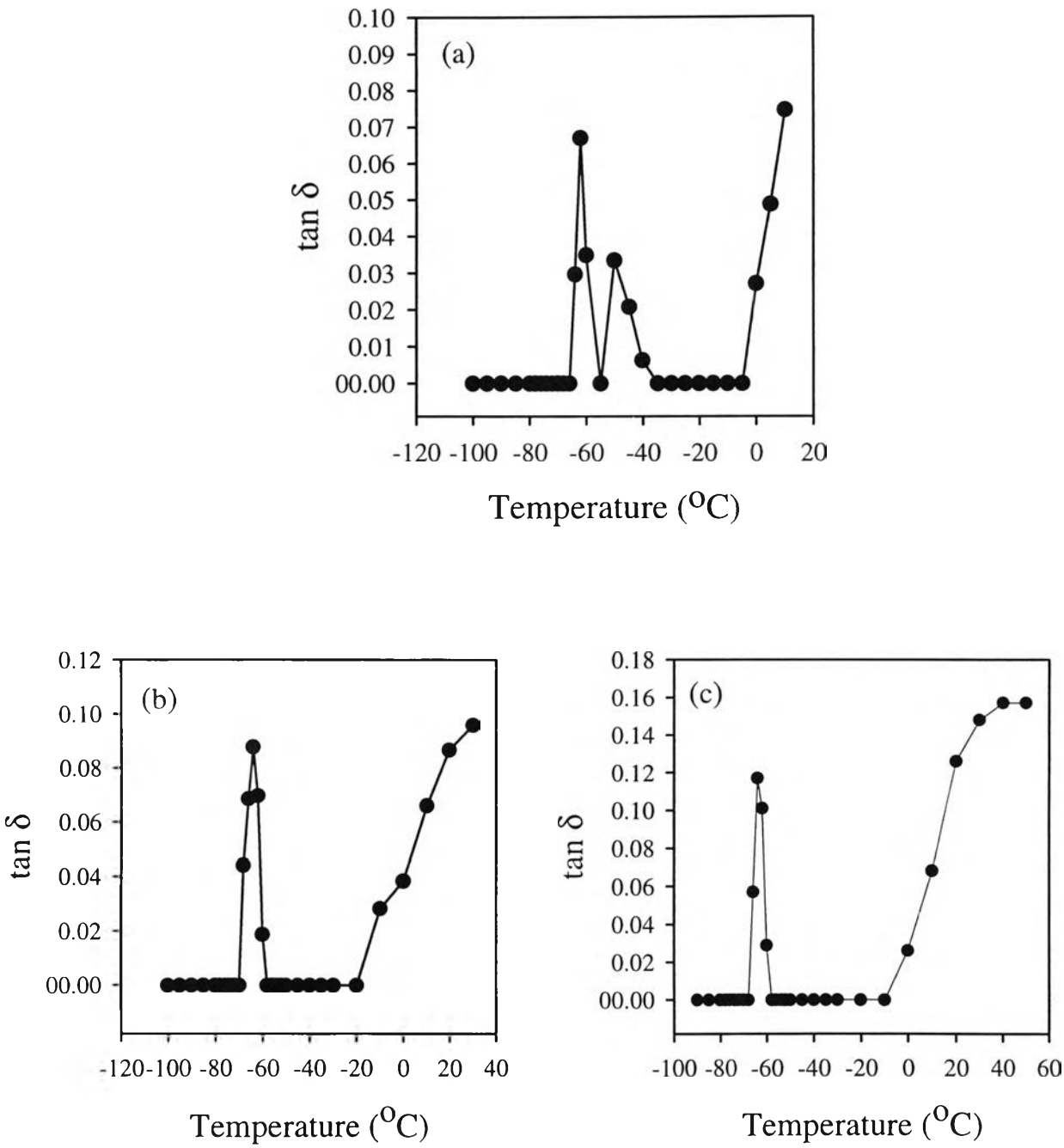

Figure 4.5 Effect of temperature on damping (tanδ) of 70/30 LLDPE/NR blend with different %maleic anhydride, (a) 3%MA, (b) 5%MA and (c) 7%MA.

4.1.1 Effect of compatibilizer on the glass transition temperature of 70/30 LLDPE/NR blends

The addition of suitably selected compatibilizers to immiscible blends should (1) reduce the interfacial energy of the phases, (2) permit a finer dispersion while mixing, (3) provide a measure of stability against gross phase segregation, and (4) result in improved interfacial adhesion (D. R. Paul, 1979). The effect of maleic anhydride as a compatibilizer on the dynamic mechanical properties of 70/30 LLDPE/NR blends is shown in Figure 4.5a-c. The two separated tanδ peaks occurred at –62 and –50°C when 3%wt maleic anhydride is added to the blend (Figure 4.5a). These separated two peaks corresponding to the glass transition temperatures of NR and LLDPE indicate that the blends are incompatible. However, the further addition of maleic anhydride can improve the compatibility of these blends, which is evident from the presence of single glass transition peak at –64°C in Figure 4.5b-c. This indicates that an incompatible LLDPE/NR blend becomes compatible miscible by the addition at a certain amount of maleic anhydride.

4.2 Morphology study

The morphology of heterogeneous polymer blends depends on type of polymer blend composition, viscosity of individual components and processing history. Danesi and Porter (1978) have shown that for blends with the same processing history, the morphology is determined by the melt viscosity ratio and composition. Generally, the least viscous component was observed to form the continuous phase over a larger composition range.

The scanning electron micrographs of toluene-extracted 70/30 LLDPE/NR blends are shown in Figure 4.6. The dark spots correspond to the empty holes left behind after dissolving NR in toluene. The white spots represent the insoluble LLDPE. In 70/30 LLDPE/NR blend, NR was found to be dispersed as domains in the continuous LLDPE matrix. This is due to the higher melt viscosity and lower content of NR compared to LLDPE in the blend.

4.2.1 Effect of maleic anhydride concentration on morphology.

The effect of maleic anhydride as a compatibilizer on the morphology of the 70/30 LLDPE/NR blend is shown in the SEM micrographs of Figure 4.6. The morphology of an uncompatibilized blend has been given in Figure 4.6a. Figures 4.6b-e show blends containing 1%, 3%, 5% and 7% MA compatibilizer, respectively. From the scanning electron micrographs it is seen that the size of the dispersed NR phase decreases with the addition of compatibilizers. This reduction in particle size with the addition of maleic anhydride is due to the reduction in interfacial tension between the dispersed NR phase and the LLDPE matrix. It indicates that the compatibilizer helps to induce interactions between the rubber and plastic and thereby increases the homogeneity of the blend. The average domain size was done by random measurement of the diameter of about 100 domains at random in each blend system.

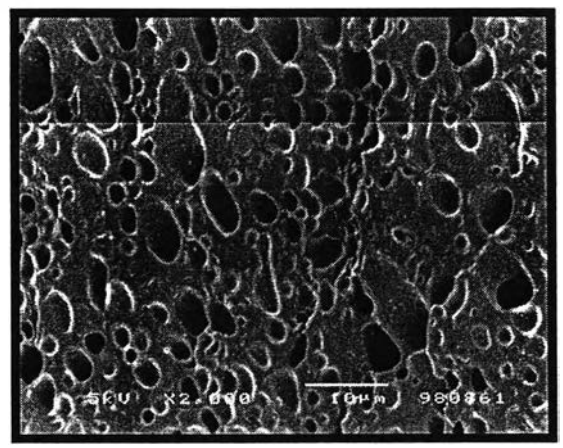

(a) 0%MA

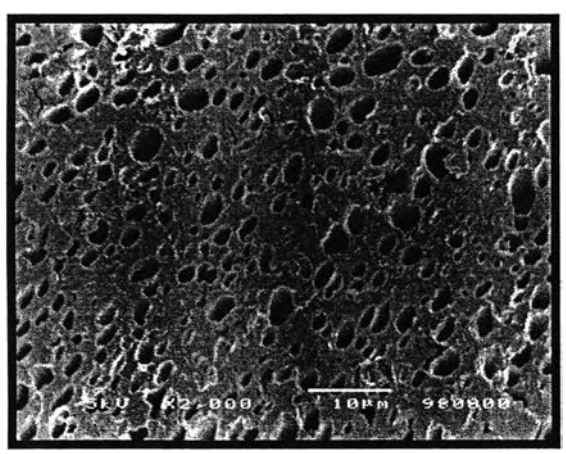

(b) 1%MA

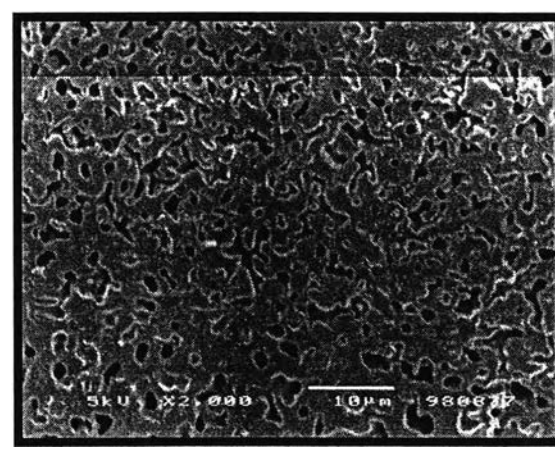

(c) 3%MA

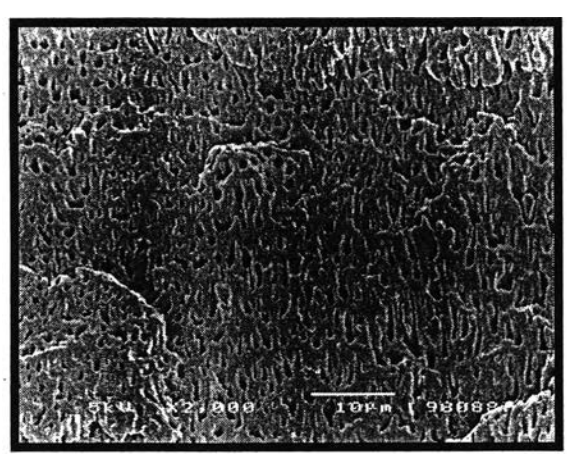

(d) 5%MA

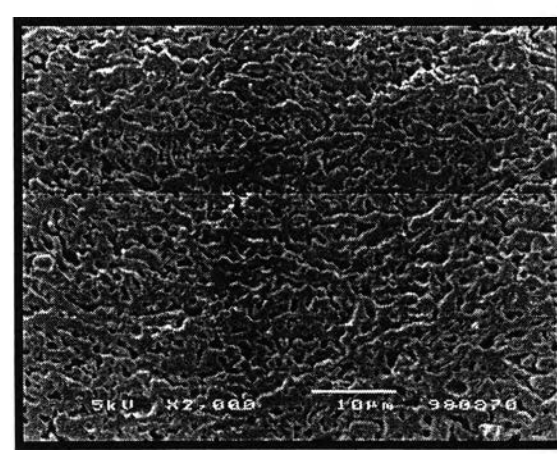

(e) 7%MA

Figure 4.6 SEM micrographs of 70/30 LLDPE/NR blends with different % maleic anhydride: (a) 0%MA, (b) 1%MA, (c) 3%MA, (d) 5% MA and (e) 7%MA.

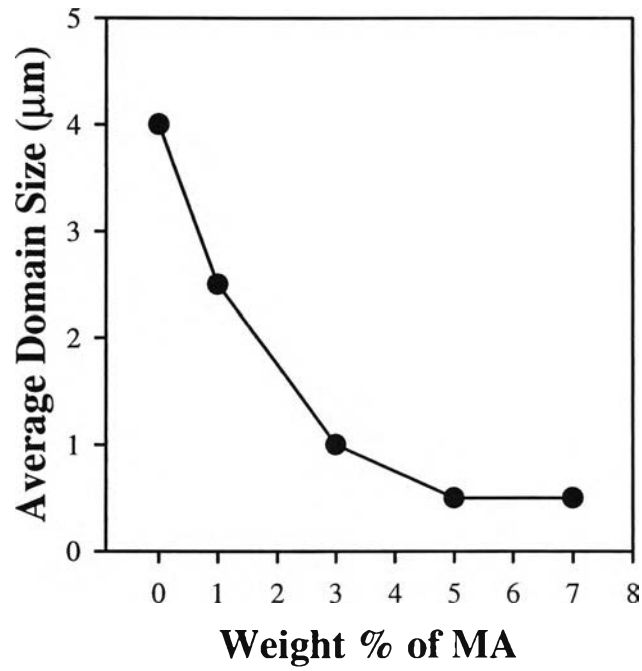

Figure 4.7 Effect of compatibilizer loading on the dispersed phase size of 70/30 LLDPE/NR blends.

Figure 4.7 shows the plot of the averaged domain size for the blends as a function of the compatibilizer content. The averaged domain size of the unmodified blend is 4 μm while in the case of compatibilized blends, the average diameter of the dispersed NR phase decreases up to the addition of 5%wt MA and is leveling off at higher concentrations of compatibilizer. By the addition of 5%wt MA, the domain size is reduced by 88% by comparison with the domain size of the unmodified blend. The equilibrium concentration at which the domain size leveled off can be considered as the so-called critical micelle concentration (CMC), i. e., the concentration at which micelles are formed. The CMC has been estimated by the intersection of the straight lines at the low and high concentration regions and is found to be 3.9% for 70/30 LLDPE/NR blend system. The CMC value indicates the critical amount of

compatibilizer required to saturate the unit volume of the interface. Several authors have reported on the interfacial saturation of binary polymer blends by the addition of compatibilizers. Thomas and Prud'homme (1992) reported that in polystyrene/poly (methyl methacrylate) blends at lower concentrations of copolymer, the dispersed phase size decreased linearly with increasing copolymer concentration, whereas at higher concentration, it leveled off. Noolandi and Hong suggested that a critical concentration of compatibilizer is required to saturate the interface of a binary blend. Above this critical concentration the compatibilizer may not modify the interface any more, but forms compatibilizer micelles in the bulk phase.

The morphology observed in SEM micrographs and the single glass transition peak observed in dynamic mechanical analysis indicates that the compatibility of LLDPE/NR blend can be improved by the addition of maleic anhydride.

4.2.2 Effect of shear force on the morphology of uncompatibilized blends

When two incompatible molten polymers are subjected to the shear force in a given flow field, droplets of one phase are produced within the other. It should be pointed out that the size of droplets has a great effect on the stability of a dispersed system. There is a tendency for small droplets to coalesce giving rise to large droplets. Hence the ability to control droplet size in flow is very important for maintaining stable flow behavior and for keeping the given process under control.

The SEM micrographs of 90/10 LLDPE/NR blends without maleic anhydride are shown in Figure 4.8a-d. The samples were prepared in dynamic single step default test of cone-and-plate rheometer at different frequencies. In Figure 4.8a, the sample was taken after being subjected to the dynamic shear at 0.1rad/sec, the NR dispersed phase is in a form of spherical droplets with diameter of about 4 μm in the LLDPE matrix. Figure 4.8b shows the

micrograph of a sample taken after being subjected to the dynamic shear at 1 rad/sec. It shows that the NR dispersed phase is elongated in the form of fibrils. When a specimen was subjected to dynamic shear force in cone-and-plate rheometer at 100 rad/sec, long fibrils of the dispersed NR phase are seen along the flow direction (Figure 4.8d). It is of interest to observe that the areas of some dispersed NR phase in Figure 4.8d are much larger than those in Figure 4.8c. This appears to suggest that the coalescence between the elongated NR droplets occurred. The fibrils like structure was also found in other polymer blend where viscosity ratio (λ) is greater than 1; for example that reported by Borisenkova *et al* (1991). They concluded that at a condition of $\lambda = 1$ fibrillar structure was pronounced, while at $\lambda < 0.2$, these fibers transformed into layers. Tsebrenko (1983) studied the influence of the viscosity ratio of melt components of polyoxymethylene/ethylene and vinyl acetate copolymer mixture on the process of fiber formation in extrudates. He found that ultrathin fibers were the sole type of structure when the viscosity ratio was close to unity. If viscosity ratio exceeded unity, the extrudates contained short fibers. If viscosity ratio was lower than 1 films were formed along with fibers. Figure 4.9 shows the plot of viscosity ratio for LLDPE/NR blend system as a function of frequency. The micrographs of 70/30 LLDPE/NR blends without maleic anhydride also show the same trend (Figure 4.10a-d) as in the 90/10 LLDPE/NR blends. It is of interest to observe the different sizes of the dispersed NR phase between 90/10 and 70/30 LLDPE/NR blends (comparing Figure 4.8a and Figure 4.10a). The bigger particle size of the rubber phase with increase in rubber content is attributed to the reagglomeration or coalescence of the dispersed rubber particles. The occurrence of coalescence at higher concentration of one of the components has been reported by many authors. S. George *et al.* (1995) showed that as the rubber content in the NBR/PP blend increases from 30 to 50wt% NBR, the average size of the dispersed NBR phase increases from 5.87 to 17.90 μm.

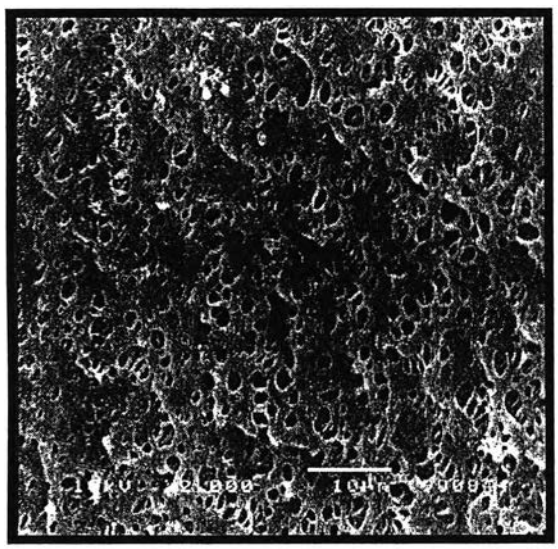

(a) 0.1 rad/sec

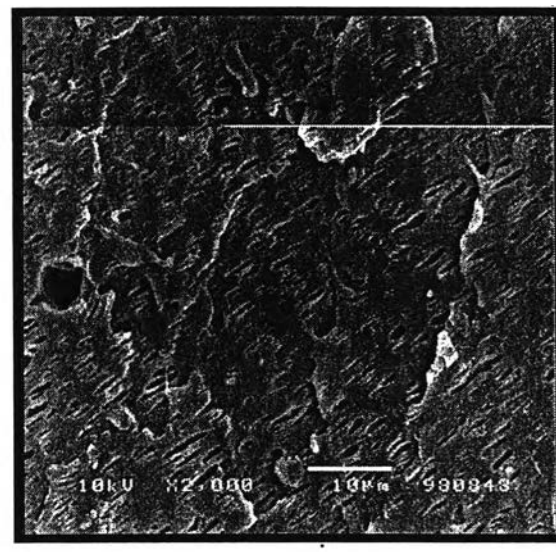

(b) 1 rad/sec

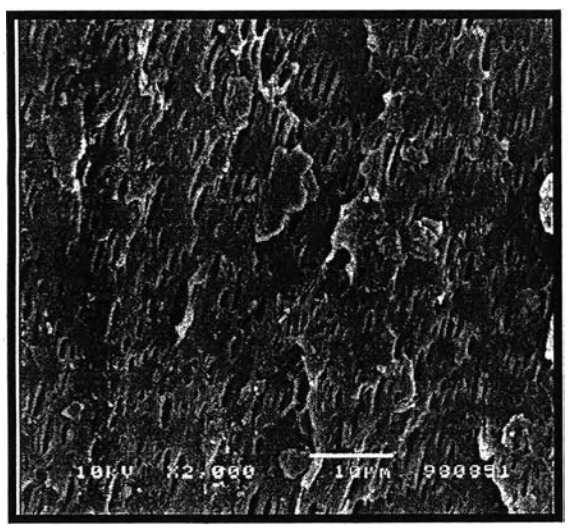

(c) 10 rad/sec

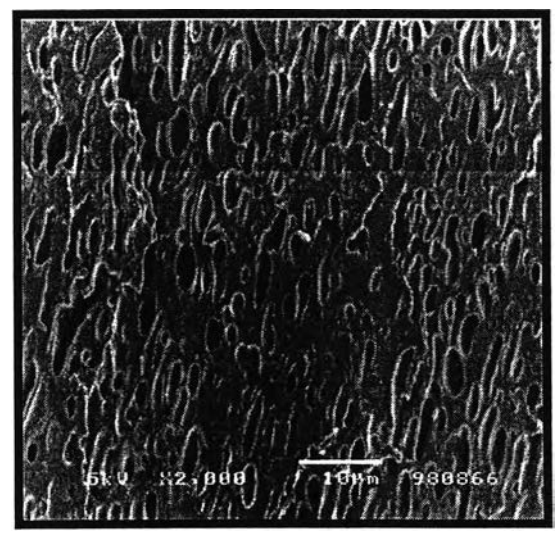

(d) 100 rad/sec

Figure 4.8 SEM micrograph of 90/10/0 LLDPE/NR/MA blends at different frequency; (a) 0.1 rad/sec, (b) 1 rad/sec, (c) 10 rad/sec and (d) 100 rad/sec at 180°C.

The drop coalescence of uncompatibilized blends also occurred in the capillary rheometer, in which the sample was subjected to the steady shear force. The effect of steady shear in capillary rheometer on the morphology of uncompatibilized 70/30 LLDPE/NR blends are shown in Figure 4.11a-b. After sample was subjected to shear at 45 1/sec, the dispersed NR is in the form of droplets which tend to coalesce together after being subjected to shear at 130 1/sec (P. Moteplay, 1999).

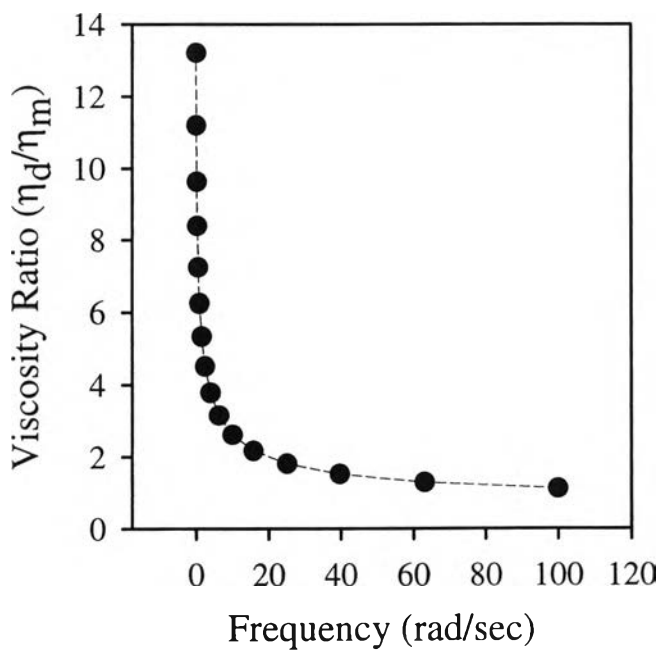

Figure 4.9 Plot of viscosity ratio for LLDPE/NR blend system as a function of frequency at 180°C.

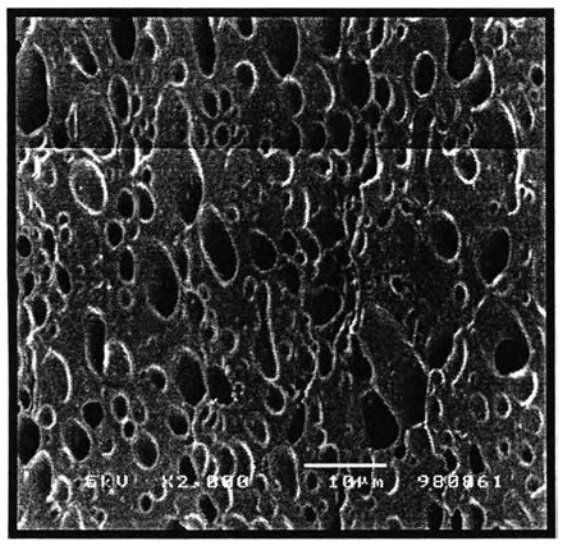

(a) 0.1 rad/sec

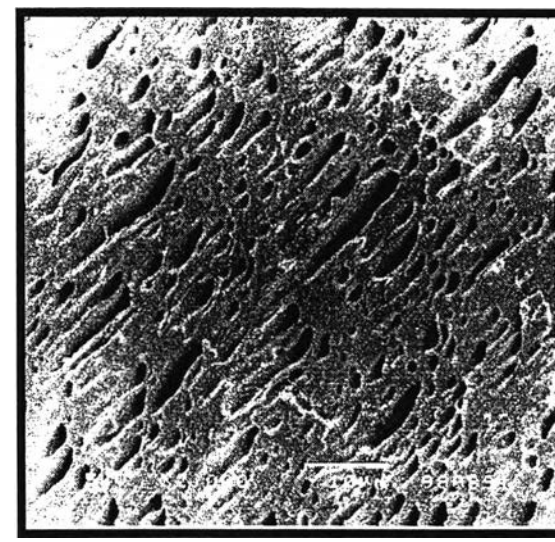

(b) 1 rad/sec

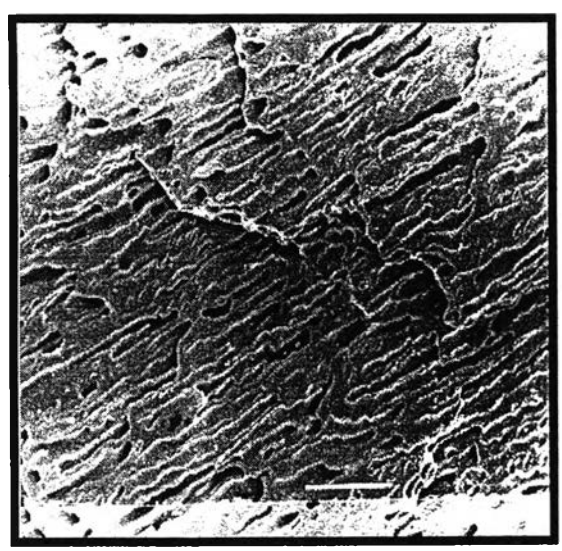

(c) 10 rad/sec

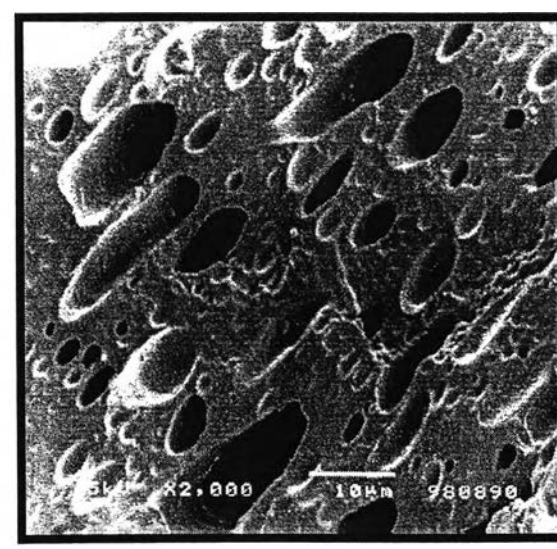

(d) 100 rad/sec

Figure 4.10 SEM micrograph of 70/30/0 LLDPE/NR/MA blends at different frequency; (a) 0.1 rad/sec, (b) 1 rad/sec, (c) 10 rad/sec and (d) 100 rad/sec at 180°C.

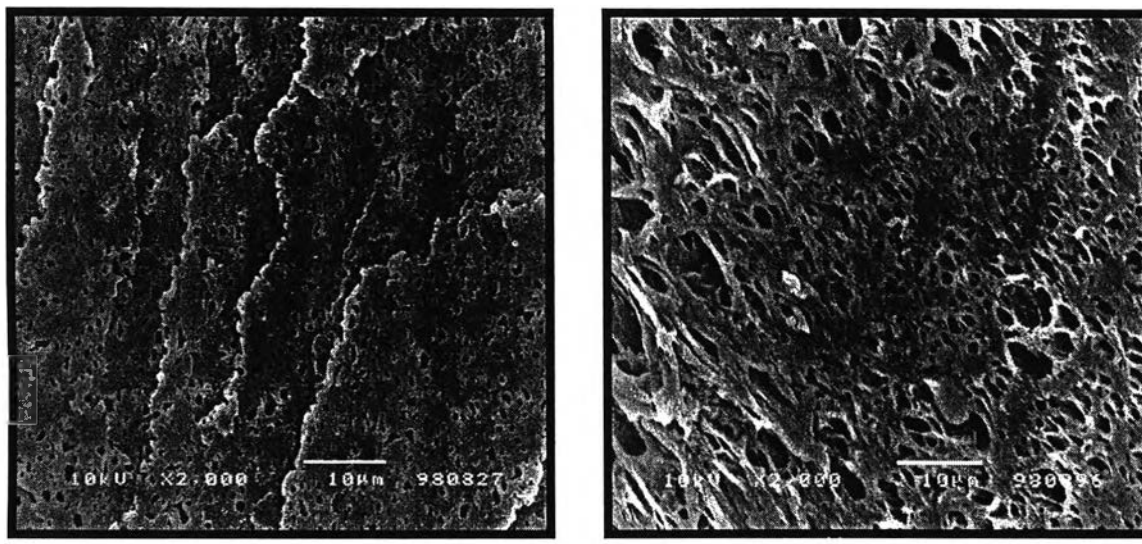

(a) 45 sec^{-1} (b) 130 sec^{-1}

Figure 4.11 SEM micrograph of 70/30/0 LLDPE/NR/MA blends at different shear rates; (a) 45 sec^{-1}, (b) 130 sec^{-1} at 180°C (P. Moteplay, 1999).

4.2.3 Effect of shear force on the morphology of compatibilized blends

The SEM micrographs of compatibilized blends are shown in Figure 4.12a-d and 4.13a-d for 90/10/3 and 70/30/5 LLDPE/NR/MA blends respectively. Figure 4.12a and 4.13a show that the morphology of NR dispersed phase after being sheared in a cone-and-plate rheometer at 0.1 rad/s is in the form of small droplet. Figure 4.12b and 4.13b give micrographs for 90/10/3 and 70/30/5 LLDPE/NR/MA blends after being subjected to higher dynamic shear force. The SEM micrographs of fracture surface indicate that the NR dispersed phase is elongated in the form of fibrils along the flow direction. However, when the blends are subjected to dynamic shearing force in cone-and-plate rheometer at 100 rad/sec, little change in morphology is observed as compared to the morphology of the specimen after being subjected to dynamic shearing force at 10 rad/sec (compare Figure 4.12c with Figure 4.12d and Figure 4.13c with 4.13d). The micrographs of 70/30/5 LLDPE/NR/MA blends, which are extruded from a capillary rheometer at shear rates of 42 and 127 1/sec, are shown in Figure 4.14a and 4.14b respectively. They show that the morphology of NR dispersed phase does not change with shear rate (P. Moteplay, 1999). Gonzalez-Nunez *et al.* studied the deformation of nylon drops in polyethylene with and without an interfacial agent, in an extensional flow. They found that at low shear stress, there is no significant deformation and the dispersed phase can be assumed to be spherical. At high shear stress the drops are deformed to ellipsoids and are aligned in the direction of the flow. When an interfacial agent is added to the system the drop deformation decreases.

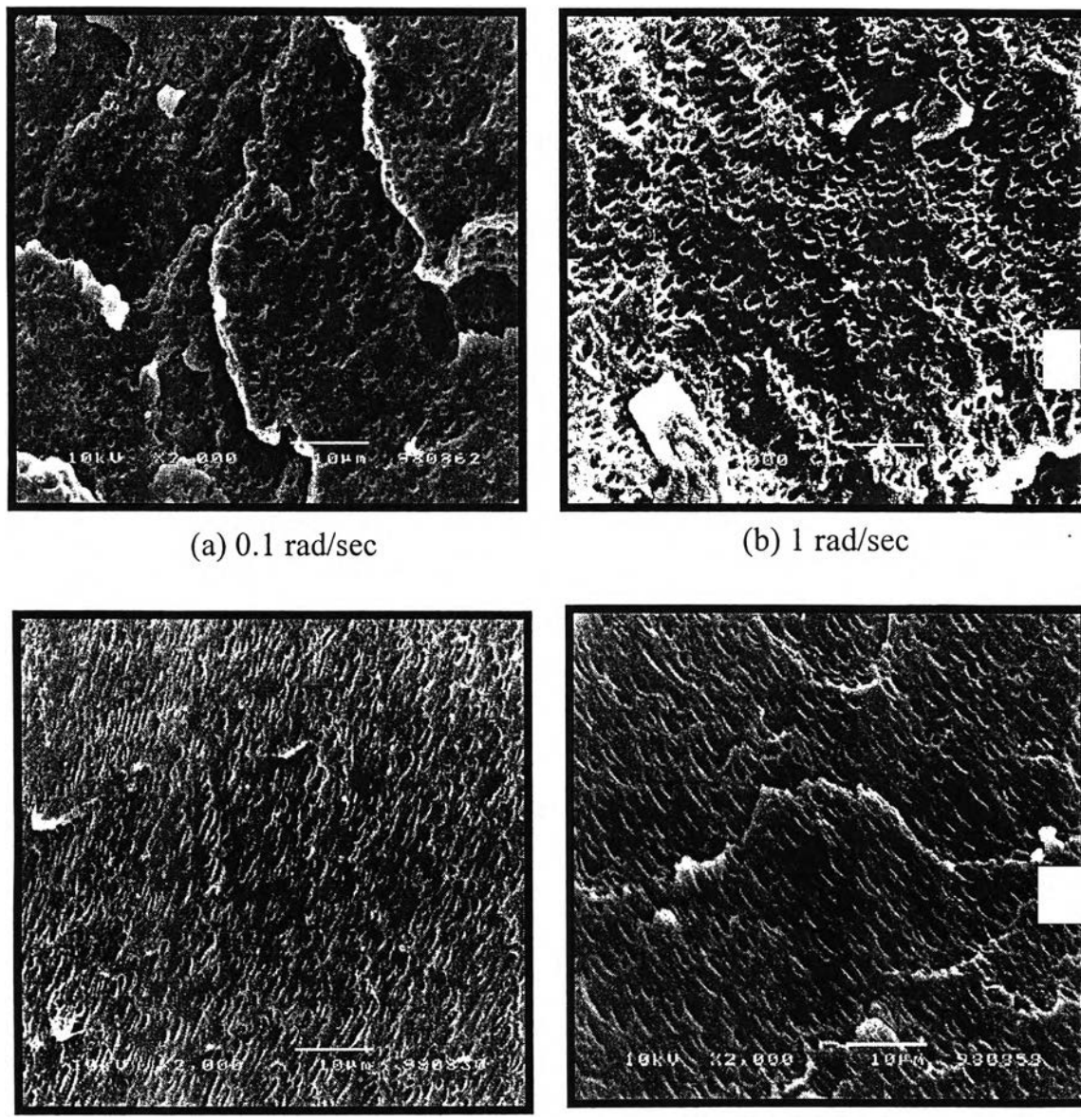

(a) 0.1 rad/sec (b) 1 rad/sec

(c) 10 rad/sec (d) 100 rad/sec

Figure 4.12 SEM micrograph of 90/10/3 LLDPE/NR/MA blends at different frequency; (a) 0.1 rad/sec, (b) 1 rad/sec, (c) 10 rad/sec and (d) 100 rad/sec at 180°C.

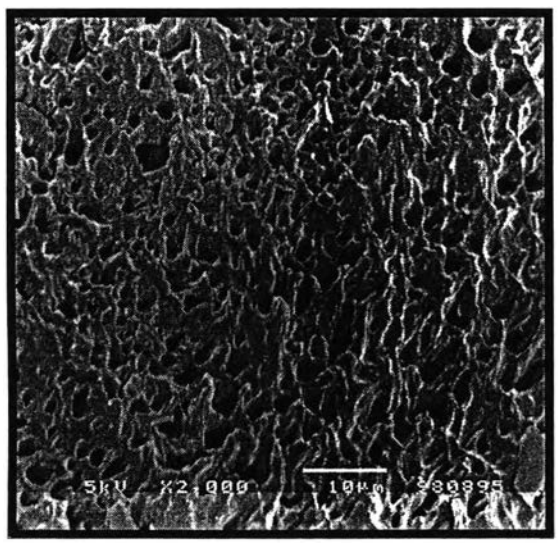

(a) 0.1 rad/sec

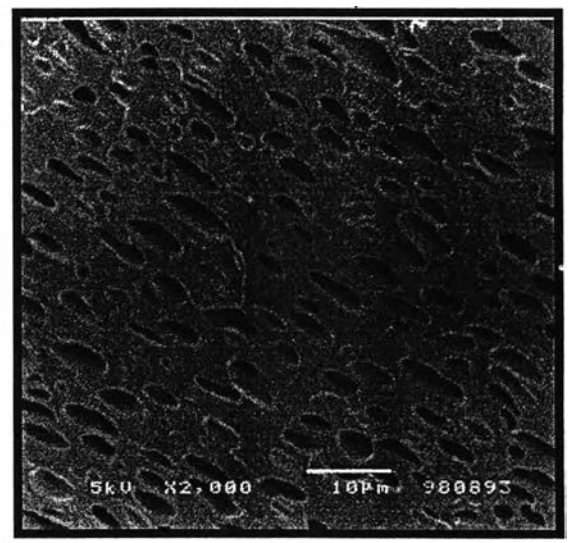

(b) 1 rad/sec

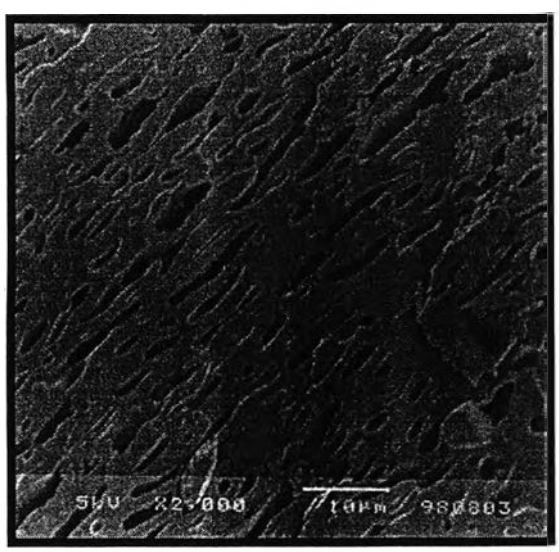

(c) 10 rad/sec

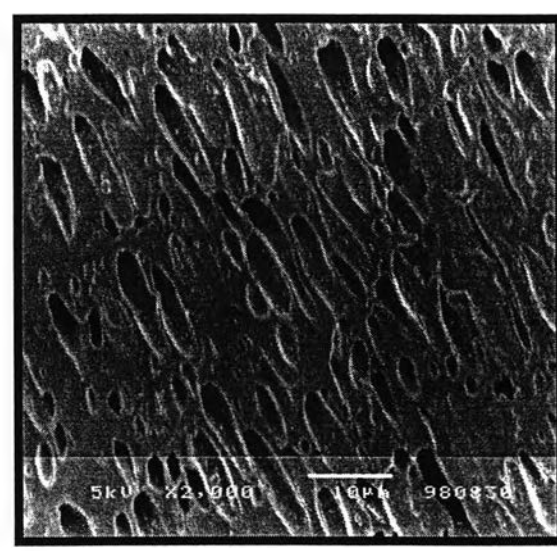

(d) 100 rad/sec

Figure 4.13 SEM micrograph of 70/30/5 LLDPE/NR/MA blends at different frequency; (a) 0.1 rad/sec, (b) 1 rad/sec, (c) 10 rad/sec and (d) 100 rad/sec at 180°C.

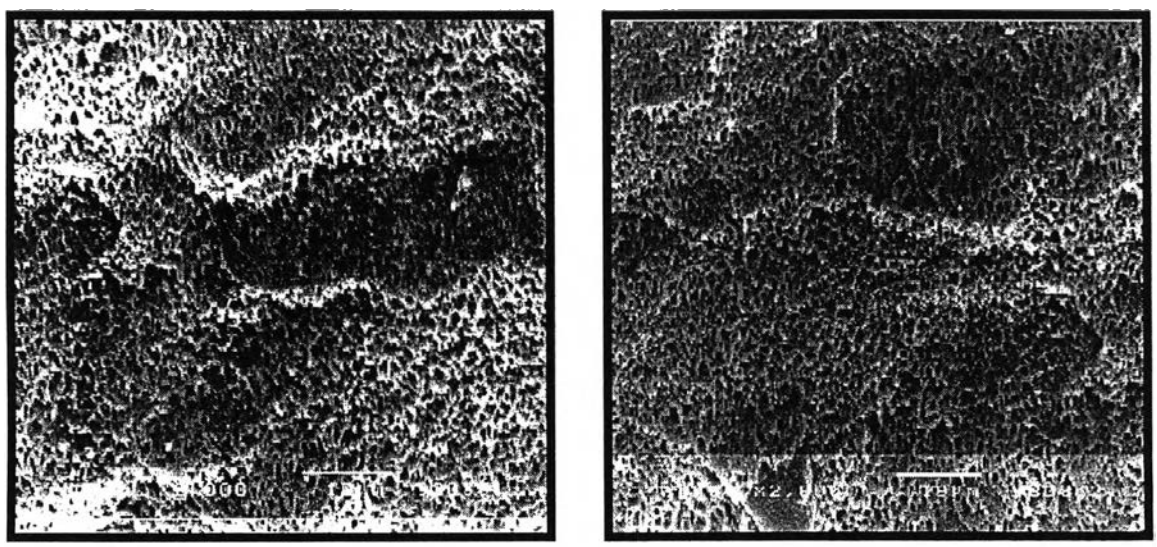

(a) 42 sec^{-1} (b) 127 sec^{-1}

Figure 4.14 SEM micrograph of 70/30/5 LLDPE/NR/MA blends at different shear rates; (a) 42 1/sec, (b) 127 1/sec at 180°C (P. Moteplay, 1999).

4.3 Rheological study

Rheological testing provides a precise means for measuring dynamic mechanical properties, which can be related to material processing characteristics and performance. This work examines the rheological characteristics of natural rubber (NR)/linear low-density polyethylene (LLDPE) blends by using cone-and-plate and capillary rheometer at low frequency and high shear rate respectively.

4.3.1 Cone-and-plate Rheometer study

The linear viscoelastic properties were measured with a rheometer equipped with a convection oven. For this study, the cone-and-plate configuration was used in dynamic mode. This dynamic test was run in the frequency range from 0.1-100 rad/sec. Test temperatures were 140, 160 and 180°C

Usually, the rheological properties of a viscoelastic material are independent of strain up to a critical strain level. Beyond this critical strain level, the material's behavior is nonlinear and the modulus declines. So, measuring the strain amplitude dependence of the storage and loss modulus (G', G") is usually the first step taken in characterizing viscoelastic behavior. Figure 4.15 shows the effect of %strain on G" for LLDPE, NR and 80/20 LLDPE/NR blend at 180°C. For all samples the linear viscoelastic region was observed up to a maximum strain, γ_m. For subsequent measurements, dynamic frequency sweep default test, the values of %strain that used, γ_ω, is less than the maximum strain, γ_m.

4.3.1.1 Effect of blend ratio on the complex viscosity of LLDPE/NR blends

The dynamic viscosity as a function of the imposed frequency is shown in Figure 4.16 for the pure LLDPE, NR and their blends at different compositions. It is seen that pure LLDPE exhibits Newtonian behavior at low

frequencies while pure NR shows shear thinning in the whole range of frequencies tested. The complex viscosity of LLDPE/NR blends are in-between those of the component polymers. Their complex viscosity decreases with increasing frequency, indicating pseudoplastic nature of the blends. This occurs because the applied force disturbs the long chains of the polymer from their equilibrium position and the molecules become disentangled in the direction of the force causing a reduction in viscosity. For the study of the effect of blend ratio, the complex viscosity is plotted as a function of %wt NR.

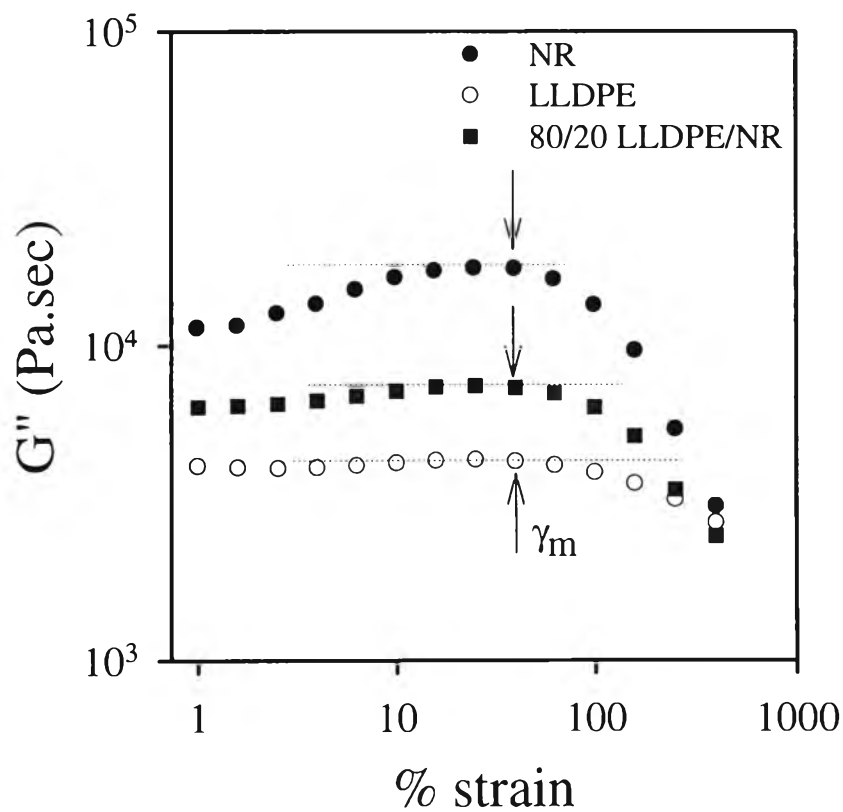

Figure 4.15 Strain sweep at 180°C for NR, LLDPE and 80/20 LLDPE/NR blend. The arrows indicate the maximum value of %strain for the linear viscoelastic response.

It is seen in Figure 4.17 that the viscosity of NR is higher than LLDPE. The differences are more prominent at low frequencies. As a function of blend composition at a constant shear rate, complex viscosity of LLDPE/NR blends varies as shown in Figure 4.17. Initially the viscosity increases up to 10wt % NR and then it drops down and finally again rises with increasing NR content beyond 30wt %. According to Han, the viscosity of immiscible polymer blends changes with their morphology and a minimum viscosity can be found at a certain blend composition when a domain can be elongated easily in the matrix. Note that in the 70/30 LLDPE/NR blend, NR become the domain structure and might be elongated easily owing to its high elasticity compared to LLDPE. It is evident that the viscosity of the blends is a nonadditive function of the viscosity of the component polymers. As the frequency increases, the differences in viscosity between the different blends narrow down.

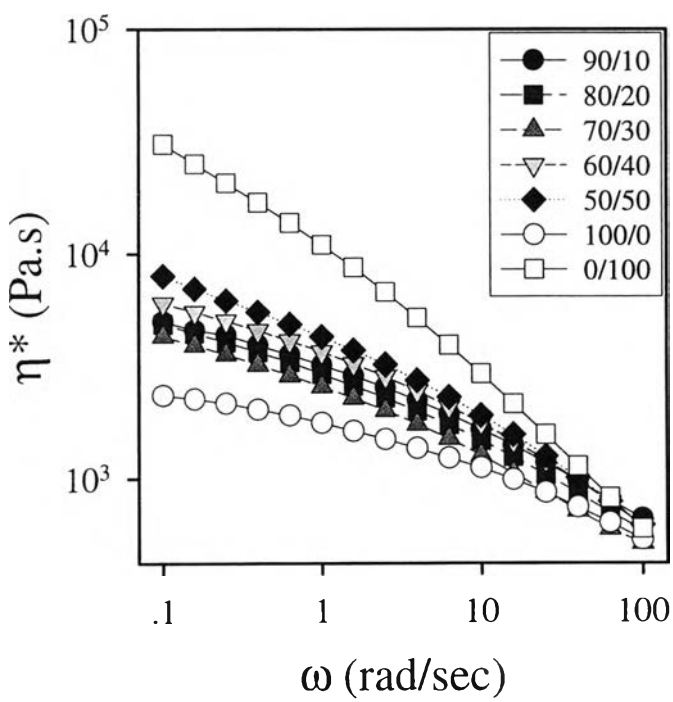

Figure 4.16 The complex viscosity as a function of frequency for pure LLDPE, NR and LLDPE/NR blends at 180°C.

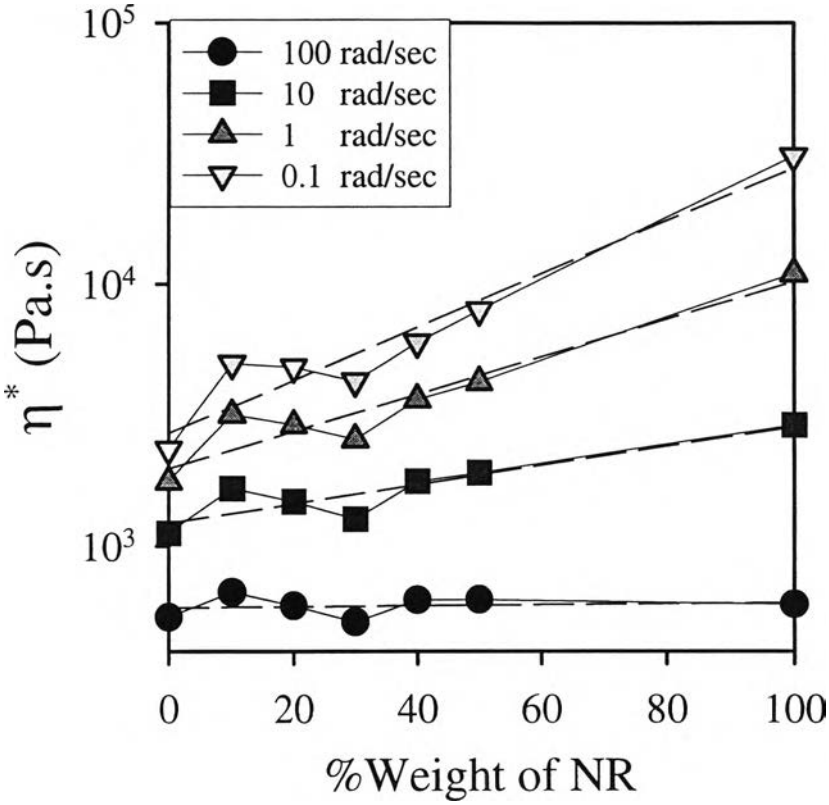

Figure 4.17 Effect of NR content on the complex viscosity of LLDPE/NR blend at various frequencies and 180°C.

4.3.1.2 Effect of maleic anhydride concentration on the complex viscosity of LLDPE/NR blends

The effect of compatibilizer (maleic anhydride) loading on the complex viscosity of 70/30 LLDPE/NR blends is shown in Figure 4.18, in which the complex viscosity is plotted against frequency at 180°C. In all cases, viscosity decreases with increasing frequency indicating pseudoplastic nature. In Figure 4.19 the complex viscosity is plotted as a function of % MA at different frequencies for 70/30 LLDPE/NR blends. It can be seen that the complex viscosity increases due to the addition of compatibilizer and slightly drops beyond 5% of MA. The effect of MA content on the complex viscosity of 90/10 and 80/20 LLDPE/NR blends at 180°C are also shown in Figure 4.20

and 4.21 respectively. For 90/10 LLDPE/NR blends system the viscosity increase with the addition of 1%wt MA and then slightly drops. In the case of 80/20 LLDPE/NR blends the viscosity increases with the addition of MA up to 3%wt and tends to decrease beyond 5%wt MA. The increase of viscosity with the addition of maleic anhydride occurred because the compatibilizer decreases the interfacial tension and hence the interaction between NR and LLDPE becomes stronger. The effect of compatibilizer on the viscosity of these blends are more pronounced in the low frequency region but at high frequency region the viscosity is unaffected by the addition of MA. The decrease of complex viscosity at a certain amount of maleic anhydride is due to the formation of micelles of the excess compatibilizer in the LLDPE matrix.

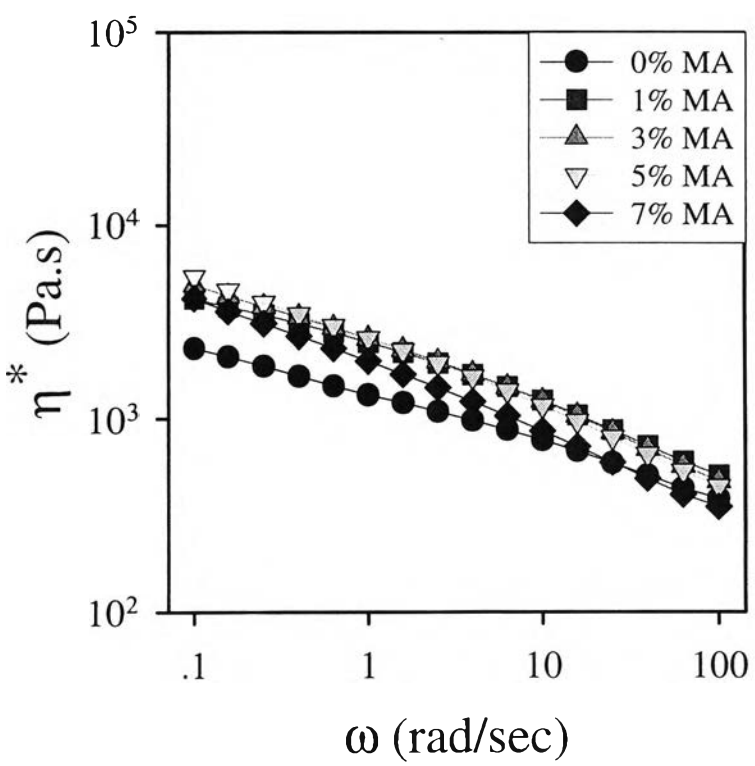

Figure 4.18 The complex viscosity as a function of frequency for 70/30 LLDPE/NR blends with various % maleic anhydride at180°C.

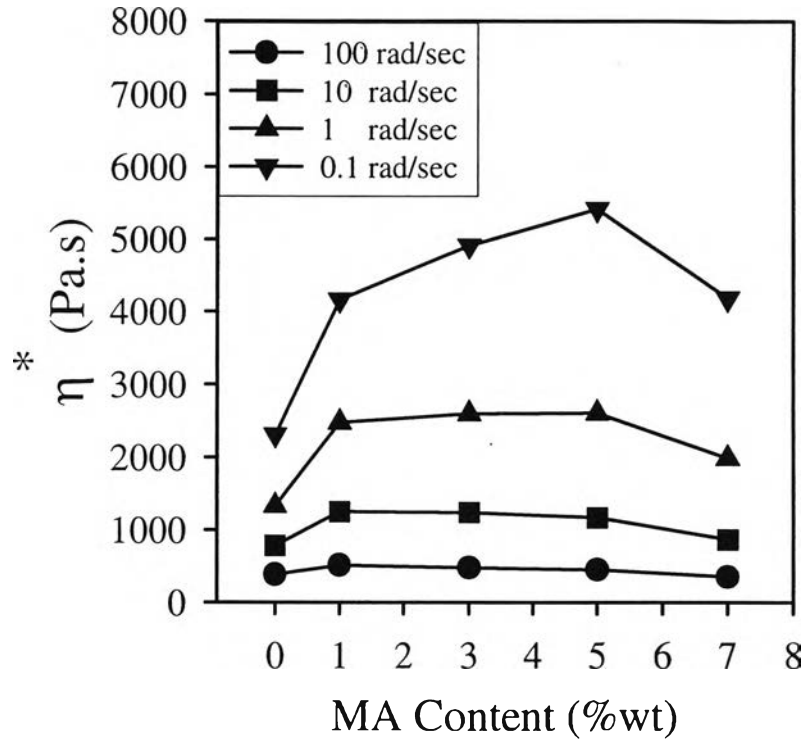

Figure 4.19 Effect of %MA on the complex viscosity of 70/30 LLDPE/NR blends as a function of frequency at 180°C.

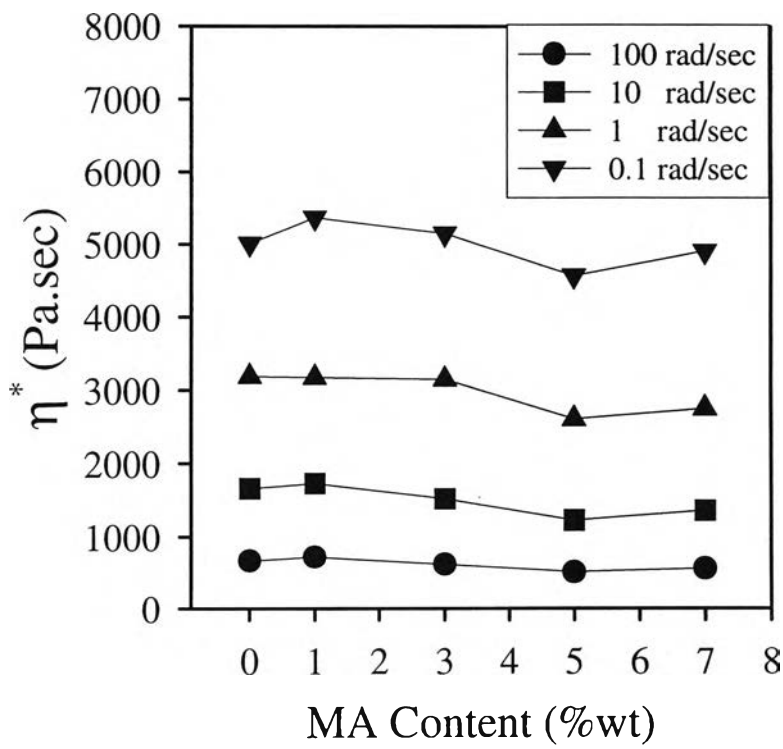

Figure 4.20 Effect of %MA on the complex viscosity of 90/10 LLDPE/NR blends as a function of frequency at 180°C.

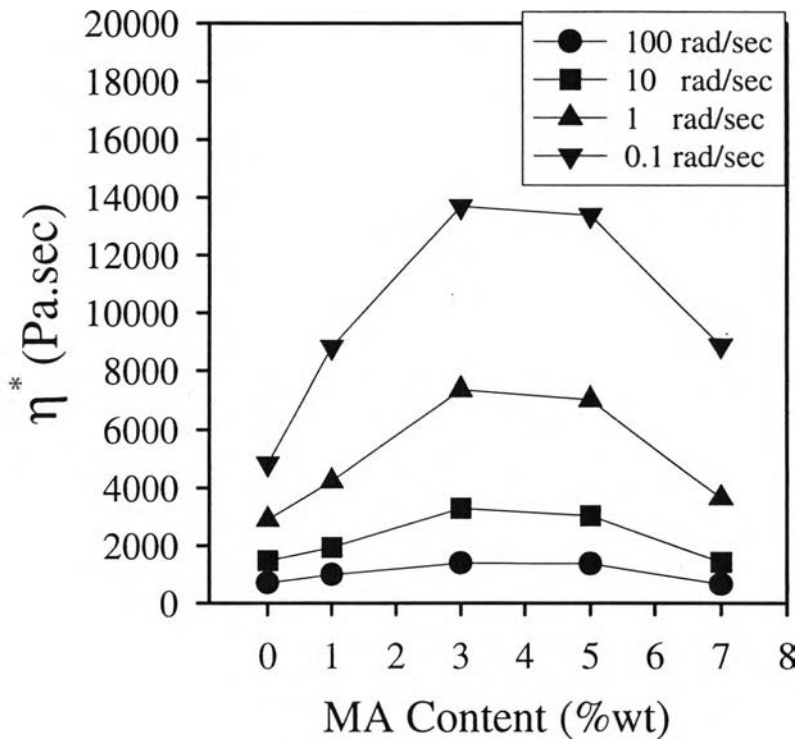

Figure 4.21 Effect of %MA on the complex viscosity of 80/20 LLDPE/NR blends as a function of frequency at 180°C.

4.3.1.3 Effect of temperature on the complex viscosity of LLDPE/NR blends

The variation of complex viscosity with temperature and frequency of uncompatibilized 70/30 LLDPE/NR blend is shown in Figure 4.22. It is clear that as temperature increases complex viscosity decreases. This follows the well-known Arrhenius behavior. Polymer chains have higher energy at elevated temperatures and this allows the material to flow more easily, thus leading to lower viscosity. The same results were found for 70/30 LLDPE/NR blend with different %MA as shown in Appendix A. Figure 4.23 is Arrhenius type plots showing viscosity-temperature dependence of uncompatibilized and compatibilized LLDPE/NR blends at frequency of 0.1 rad/sec. It is seen that the viscosity of all the blends drop with increasing temperature.

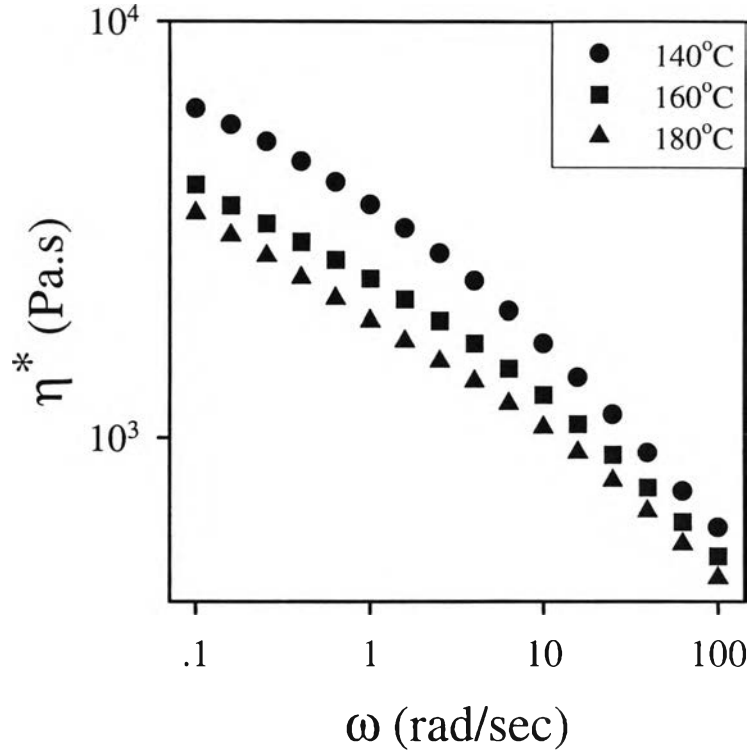

Figure 4.22 The complex viscosity as a function of frequency for 70/30 LLDPE/NR blends without maleic anhydride at different temperature.

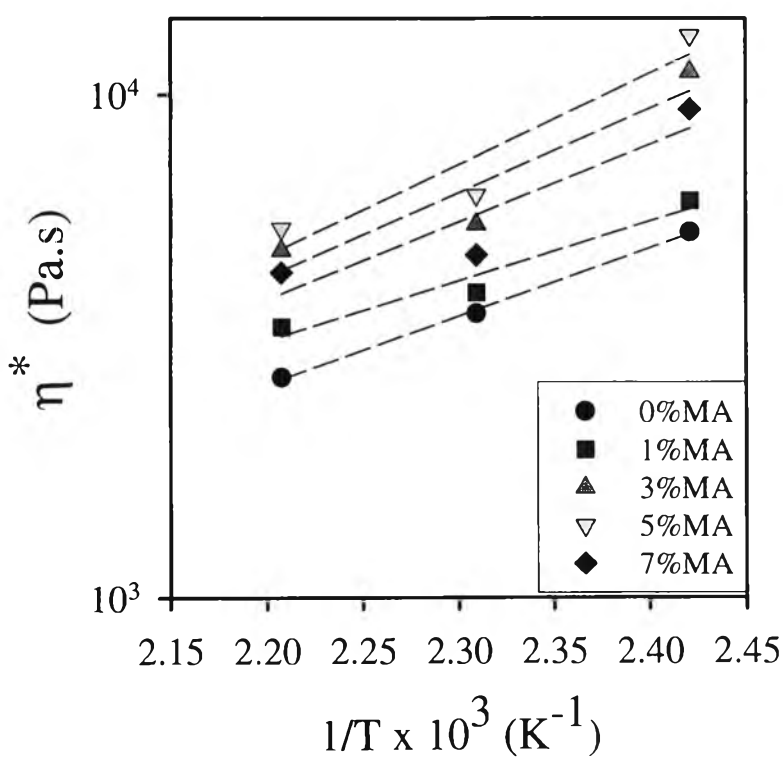

Figure 4.23 Effect of temperature on the complex viscosity of 70/30 LLDPE/NR blends with various %MA at frequency 0.1 rad/sec.

4.3.1.4 Effect of filler contents on the complex viscosity of LLDPE/NR blends

Usually, the filler is added to the thermoplastic for the reduction of production cost. Sometimes when filler particle size is small, e.g. less than 1 μm and has high structure or anisotropy, the filler (e.g. carbon black) can reinforce the matrix polymer. The effect of the addition of calcium carbonate filler on the complex viscosity of 70/30 LLDPE/NR blend is investigated by cone & plate rheometer at 180°C. The plot of complex viscosity vs. frequency for pure NR, LLDPE and 70/30 LLDPE/NR blends containing different loading of calcium carbonate is shown in Figure 4.24. The viscosity increases with increasing filler loading. This increase is more pronounced at low frequency while at high frequency all blend systems possess nearly same viscosities.

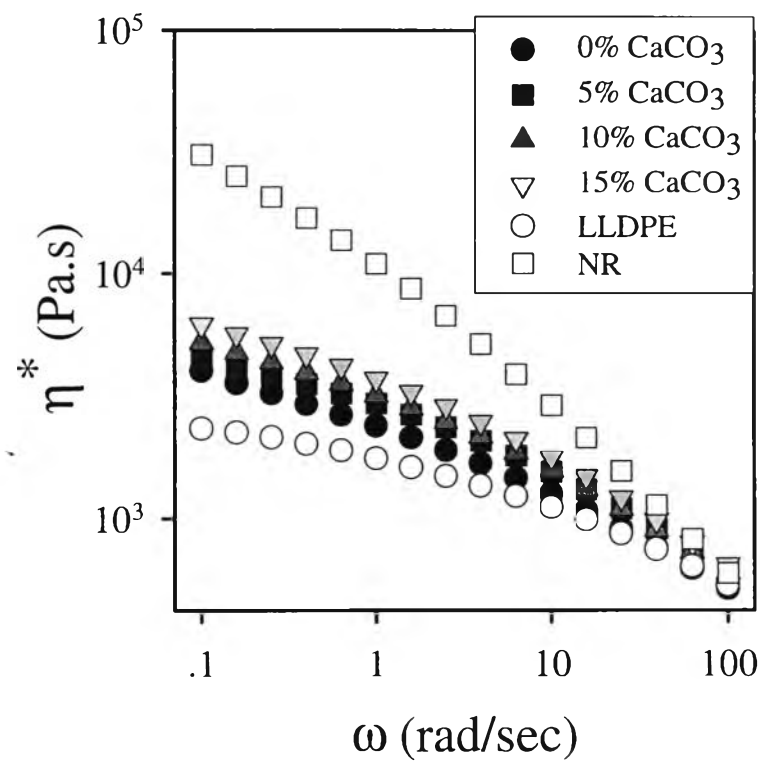

Figure 4.24 Effect of $CaCO_3$ content on the complex viscosity of 70/30 LLDPE/NR blend compare with pure components at 180°C.

4.3.1.5 Effect of blend ratio on the storage and loss modulus of LLDPE/NR blends

The dynamic moduli are the basic rheological functions obtained in dynamic experiments. The storage, G', loss, G", shear modulus at 180°C for pure LLDPE, NR, and their blends are plotted respectively as a function of frequency in Figure 4.25 and 4.26. LLDPE has G" higher than G' within the frequency range of 0.1-100 rad/sec while NR has comparable G' and G" except at high frequency > 10 rad/sec (G' greater than G"). Both G' and G" of NR are greater than those of LLDPE. Thus, when NR was added to LLDPE, the blend moduli increase with the amount of NR. Moreover, adding NR causes a faster drop of G" than G' and hence the blend becomes more elastic or toughen than LLDPE at higher frequency or shear rate. Figure 4.27 shows the variation of storage, loss and complex modulus of LLDPE/NR blends at a very low frequency of 0.1 rad/sec as a function of NR content. It is seen that the moduli increase with the increase of rubber content. This is due to the reduction in the crystalline volume of the system as increasing the concentration of NR whose elasticity is always higher than LLDPE. The increasing in complex modulus with NR content indicates that the melt strength of the blends increases with the increase of rubber content.

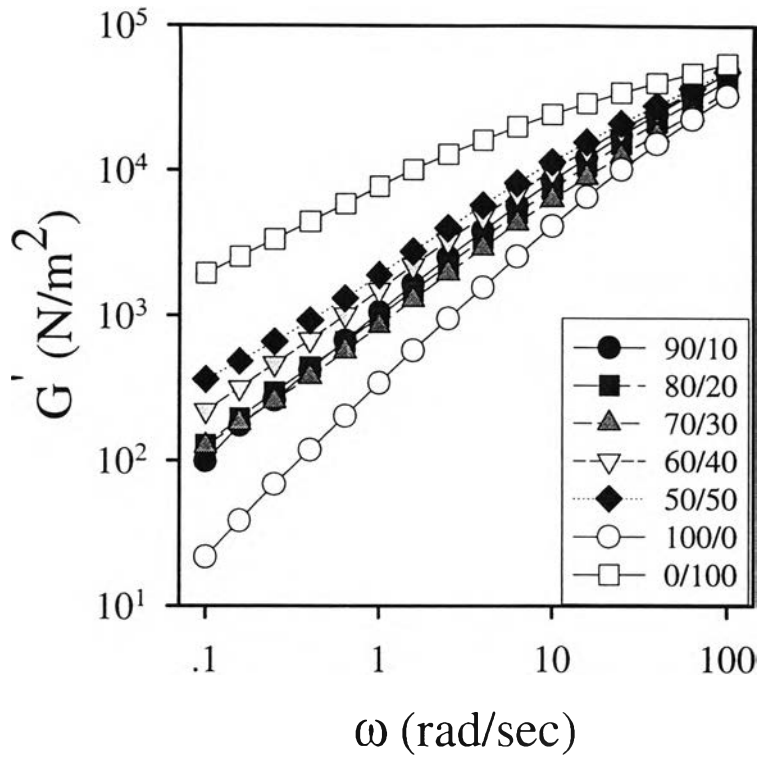

Figure 4.25. The storage modulus as a function of frequency for pure LLDPE, NR and LLDPE/NR blends at 180°C.

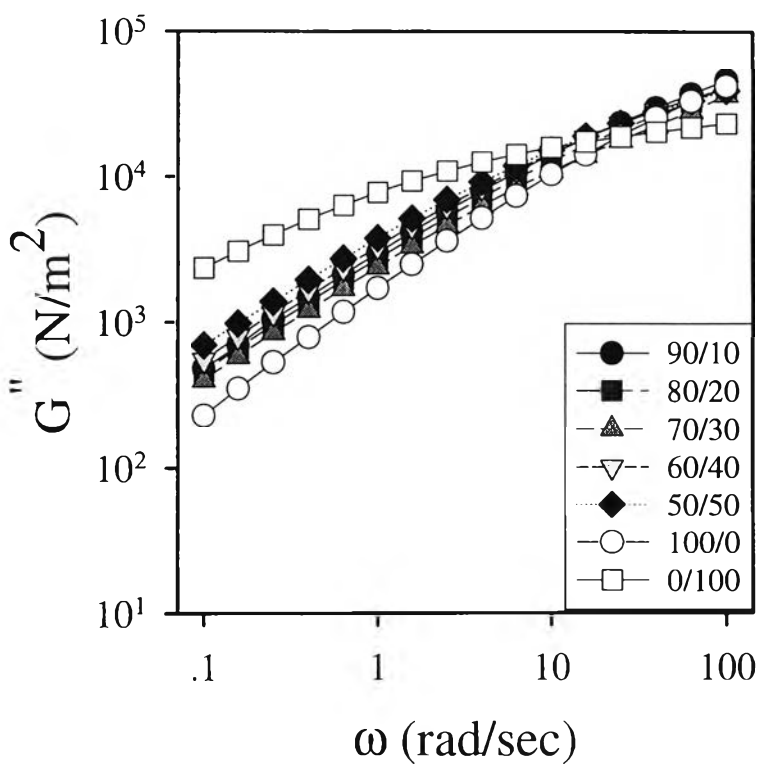

Figure 4.26. The loss modulus as a function of frequency for pure LLDPE, NR and LLDPE/NR blends at 180°C.

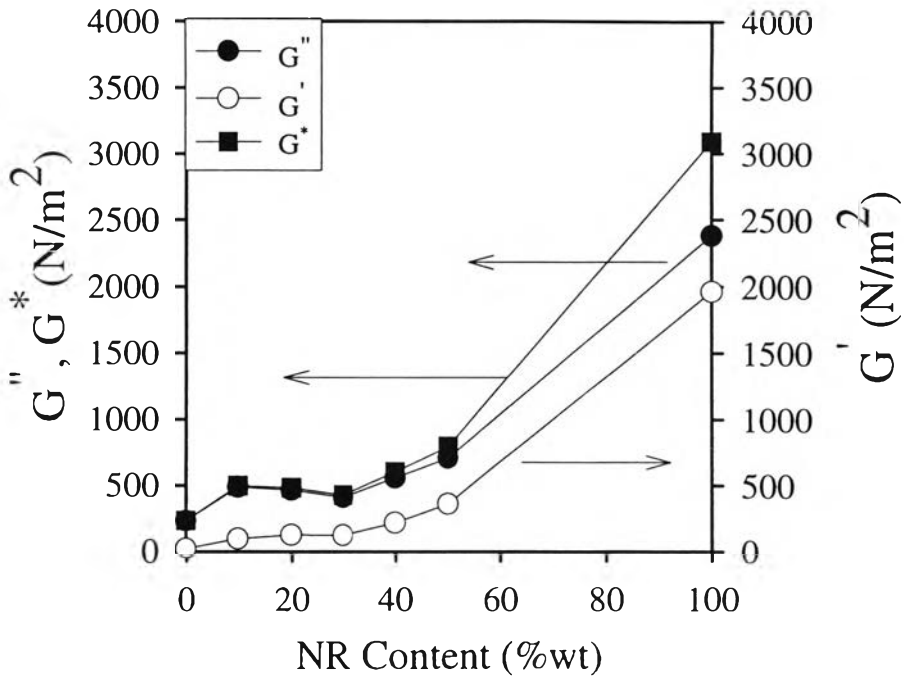

Figure 4.27. The effect of NR concentration on the storage, loss and complex modulus for LLDPE/NR blends at 180°C and frequency of 0.1 rad/sec.

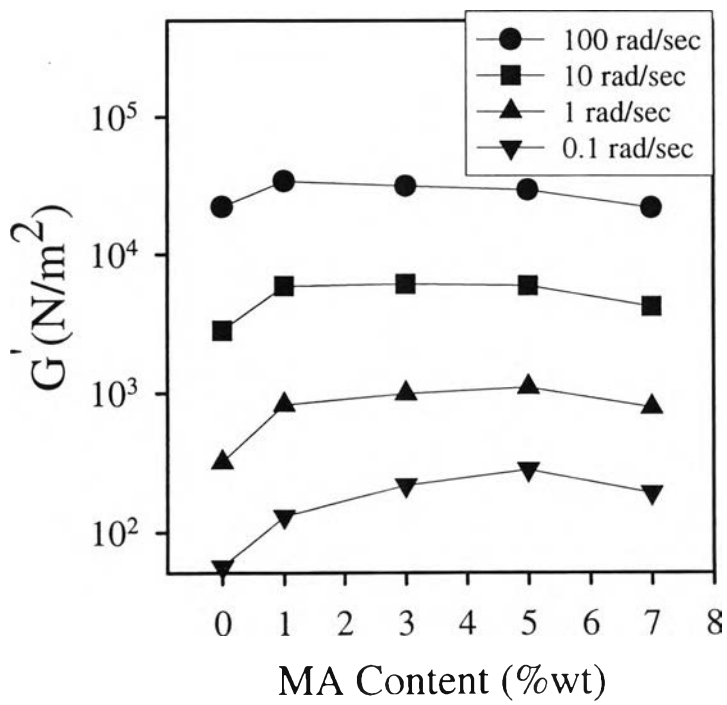

Figure 4.28. Effect of MA content on the storage modulus of 70/30 LLDPE/NR blend as a function of frequency at 180°C.

4.3.1.6 Effect of maleic anhydride on the storage modulus of LLDPE/NR blends

The variation of the storage modulus as a function of MA concentration of 70/30 LLDPE/NR blends at different frequencies is shown in Figure 4.28. With the addition of 5%wt MA the modulus of the blend increases at low frequency. However, with further addition of the compatibilizer the storage modulus rather decreases. The increase of storage modulus at low frequency implies that the elastic properties of the blend increase with the addition of maleic anhydride. This is due to the increase of the interfacial adhesion caused by the emulsifying effect of maleic anhydride, hence the interaction between LLDPE and NR phase increases. The better interaction between LLDPE and NR in the presence of MA is evident from the morphology observed in SEM micrographs. The decrease in modulus at a higher concentration of maleic anhydride is due to the micelle formation of the excess maleic anhydride. Similar behavior has been reported in the compatibilization of PP/NBR blends by Ph-PP copolymer. S. George *et al.* reported that the modulus of the PP/NBR blend increased by compatibilization using Ph-PP copolymers up to interface saturation concentration, and after that the modulus decreased. At higher frequency or shorter time scale all the blends of LLDPE/NR/MA show approximately the same modulus.

4.3.2 Capillary Rheometer study

The capillary rheometer enabled us to obtain shear viscosity at high shear rates, not obtainable with the cone-and-plate rheometer. Data presenting below are the results of steady shear viscosity obtained from capillary rheometer with the Rabinowitch correction. In this work no end corrections were applied to the shear stress data.

4.3.2.1 Effect of blend ratio, shear stress and shear rate on melt viscosity

The variation of shear viscosity with shear stress and shear rate for LLDPE, NR and their blends at 180°C is shown in Figure 4.29 and 4.30 respectively. As shear stress (or shear rate) increases, the viscosity in all cases decreases, indicating a pseudoplastic flow behavior. This occurs because the molecules are disentangled in the direction of force. It is seen that at low shear stress (or shear rate) the steady viscosity of NR is much higher than that of LLDPE. The binary blends have intermediate viscosity between the individual components. The viscosity of the blends is nonadditive function of the viscosity of the component polymers. As the percentage of NR increases, viscosity increases up to 30 %wt NR and thereafter the melt viscosity decreases slightly.

4.3.2.2 Effect of maleic anhydride, shear stress and shear rate on melt viscosity of 70/30 LLDPE/NR blends

The effects of compatibilizer loading, shear stress and shear rate on the melt viscosity of 70/30 LLDPE/NR blends at 180°C is shown in Figure 4.31 and 4.32. In all cases viscosity decreases with increasing shear stress (or shear rate) indicating pseudoplastic nature.

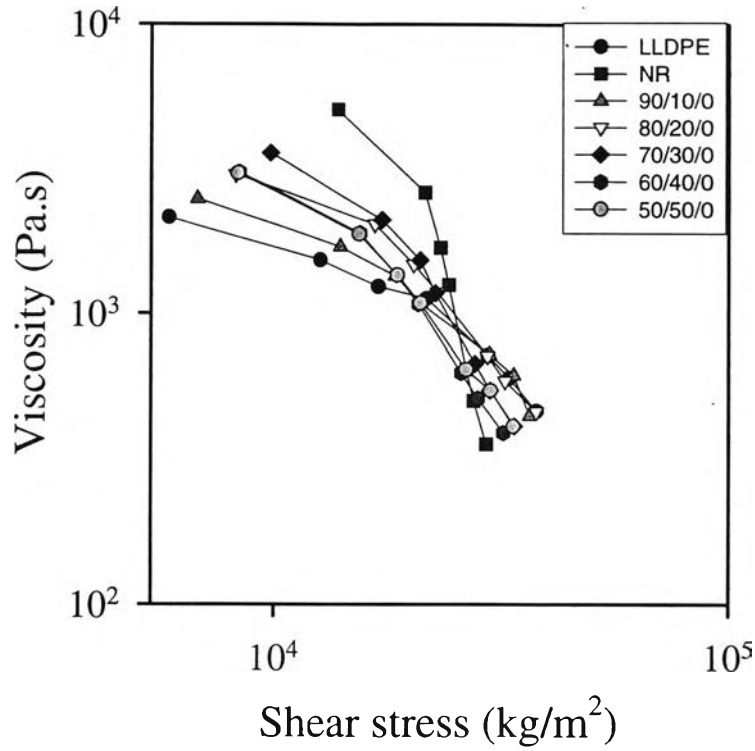

Figure 4.29. Variation of viscosity with shear stress at 180°C for LLDPE/NR blend at various compositions.

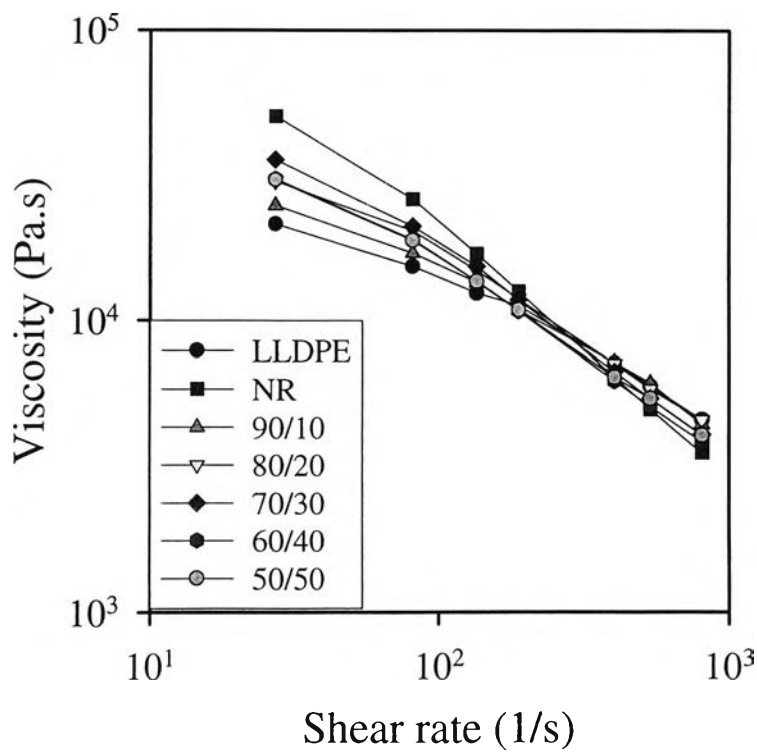

Figure 4.30. Variation of viscosity with shear rate at 180°C for LLDPE/NR blend at various compositions.

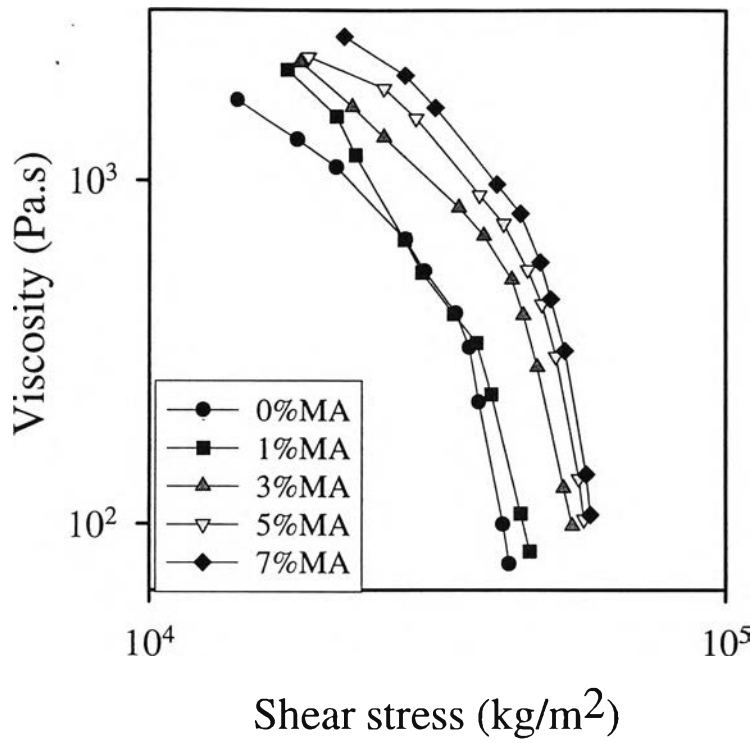

Figure 4.31 Variation of viscosity with shear stress at 180°C for 70/30 LLDPE/NR blends with various percent maleic anhydrides.

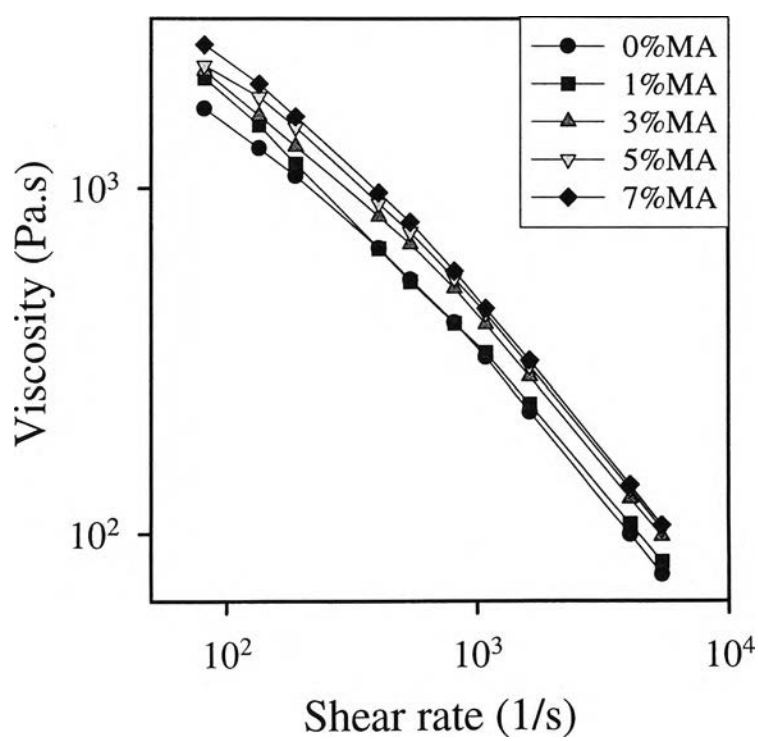

Figure 4.32 Variation of viscosity with shear rate at 180°C for 70/30 LLDPE/NR blends with various percentage of maleic anhydrides.

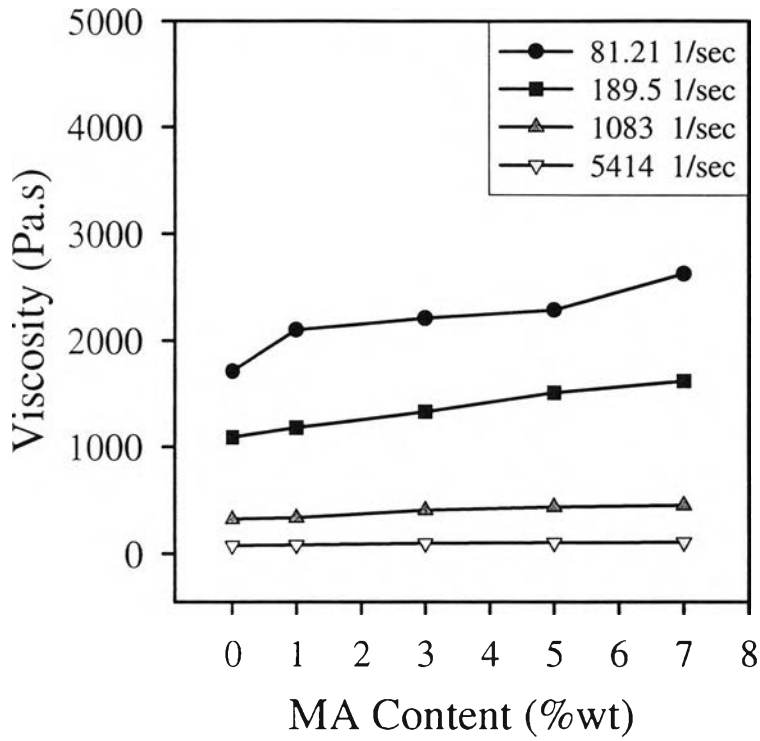

Figure 4.33 Variation of viscosity as a function of MA content for 70/30 LLDPE/NR blends at 180°C with various shear rates.

Apparent viscosity is plotted as a function of maleic anhydride concentration for 70/30 LLDPE/NR blends at different shear rates in Figure 4.33. The increasing of viscosity with maleic anhydride is due to the decreasing of interfacial tension between LLDPE and NR. The effect of compatibilizer in increasing the viscosity of LLDPE/NR blend system is more pronounced in the low shear rate region. But at high shear rates the viscosity is unaffected by the addition of maleic anhydride.

4.3.2.3 Effect of maleic anhydride on the extrudate swell of 70/30 LLDPE/NR blends at different temperatures

The swelling of an extrudate on emerging from a capillary is typical of non-Newtonian viscoelastic fluids and is related to their elastic properties. When the melt emerges from the die, reorientation of molecules occurs leading to the phenomenon of extrudate swell. The extrudate swell ratio (D_e/D) is the ratio of extrudate diameter, D_e to the capillary die diameter, D. The effect of compatibilizer on extrudate swelling is illustrated in Figure 4.34. It is seen that at 180°C the extrudate swell ratio increases sharply with increasing maleic anhydride concentration up to 5%wt and then slightly drops. This is due to an increase in the specific interaction between LLDPE and NR resulting in an increase of the elastic properties of the blends. This result is similar to the result of the effect of maleic anhydride on the dynamic storage modulus as we discussed earlier. The swelling ratio increases with the reduction of extrusion temperature. The effect of shear rate on the extrudate swell of compatibilized and uncompatibilized blends at 180°C is shown in Figure 4.35. The extrudate swell of compatibilized blend is higher than that of uncompatibilized blend at shear rates of 45 and 130 sec^{-1}. The effect of NR content on the extrudate swell of LLDPE/NR blends without MA is shown in Figure 4.36. The extrudate swell value increases sharply when the NR is added to LLDPE up to 20% wt and then slightly increases with the increase of weight % of NR. This indicate that the elasticity of the blends increase with the increasing in NR content.

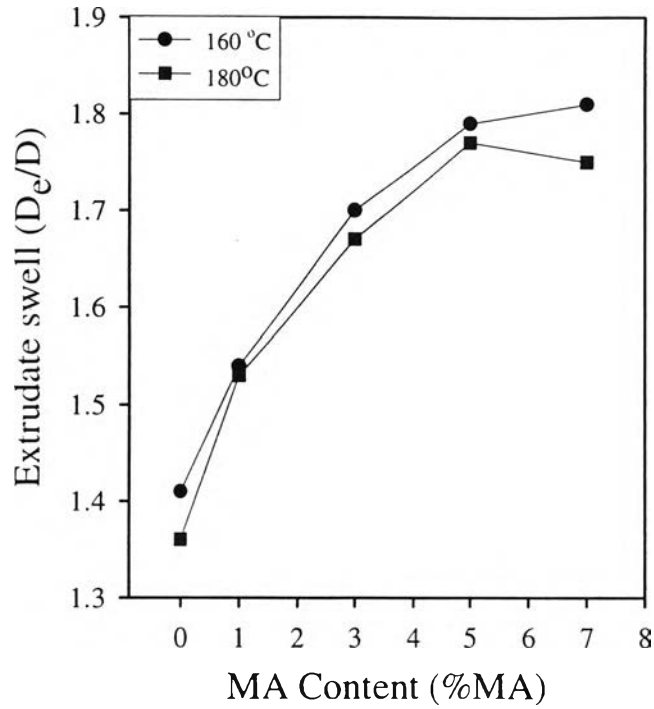

Figure 4.34 Effect of maleic anhydride concentration and temperature on the extrudate swell of 70/30 LLDPE/NR at the shear rate 45 sec^{-1}.

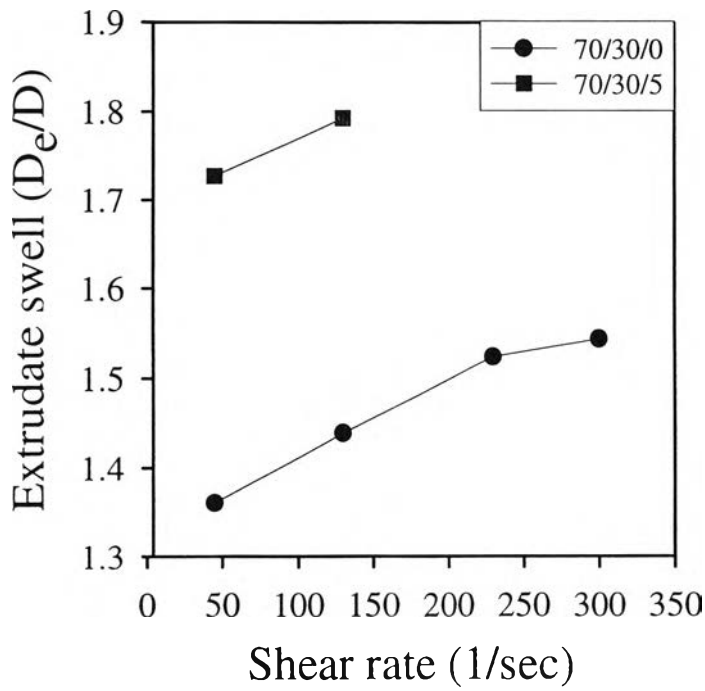

Figure 4.35 Effect of shear rate on the extrudate swell of LLDPE/NR blends with and without maleic anhydride at 180°C.

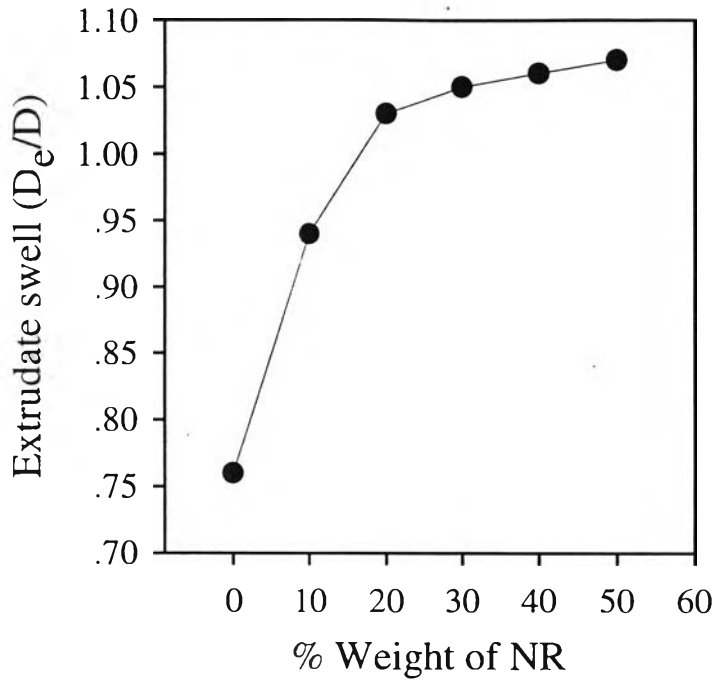

Figure 4.36 Effect of NR content on the extrudate swell of LLDPE/NR blends without MA at 180°C and shear rate 45 sec^{-1}.

4.3.3 Time-Temperature superposition

It is difficult in experiment to measure the viscoelastic properties over extended time or temperature range. For this reason the method of time-temperature superposition has been frequently used. Different isothermal spectra, each obtained over a narrow frequency, or time range, are superimposable by shifting each point of the curve by the same amount along the frequency or time axis. The method can be applied only to systems with stable morphology within the range of measured variables. Figure 4.37 shows the storage and loss modulus master curve of pure LLDPE. As can be seen, LLDPE shows good superposition of both G' and G" over a temperature range of 140 to 200°C, using a reference temperature of 180°C and shift factors a_T represented in Figure 4.38. This figure shows that the shift factor of the pure LLDPE obeys an identical Arrhenius'law, with activation energy of 33 kJ/mol.

This value is close to *Ea* = 27 kJ/mol of polyethylene which got from the literature. (S. H. Wasserman *et al.*, 1996)

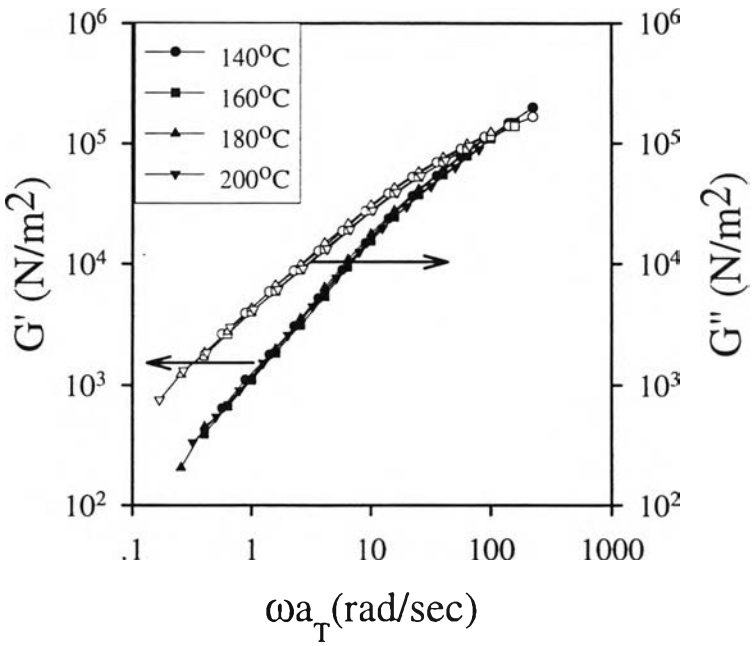

Figure 4.37 Storage and loss modulus master curve of pure LLDPE at the reference temperature 180°C.

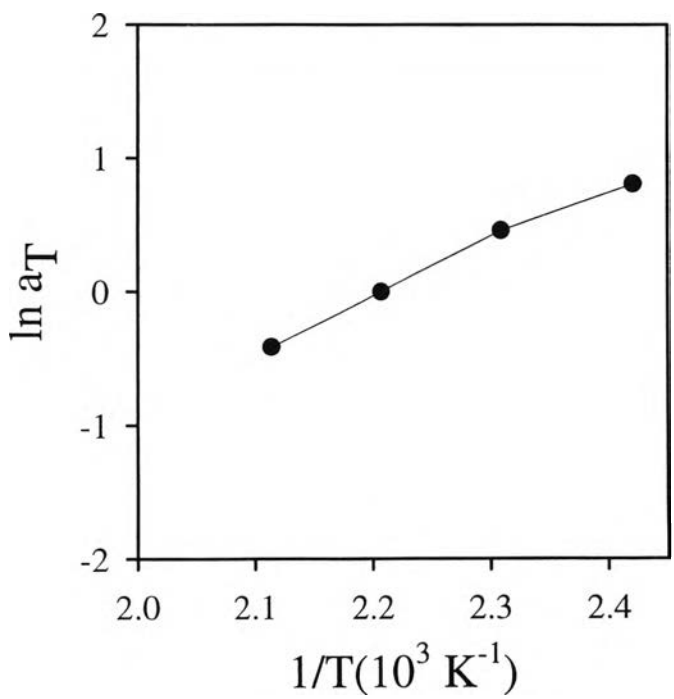

Figure 4.38 Shift factors a_T from master curves of pure LLDPE at the reference temperature 180°C.

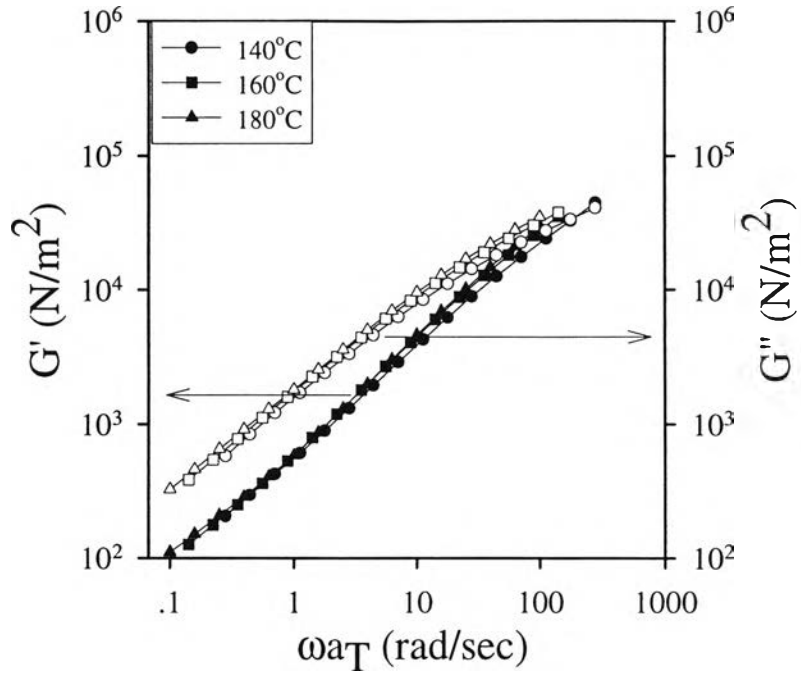

Figure 4.39 Storage and loss modulus master curve of 70/30 LLDPE/NR blend at the reference temperature 180°C.

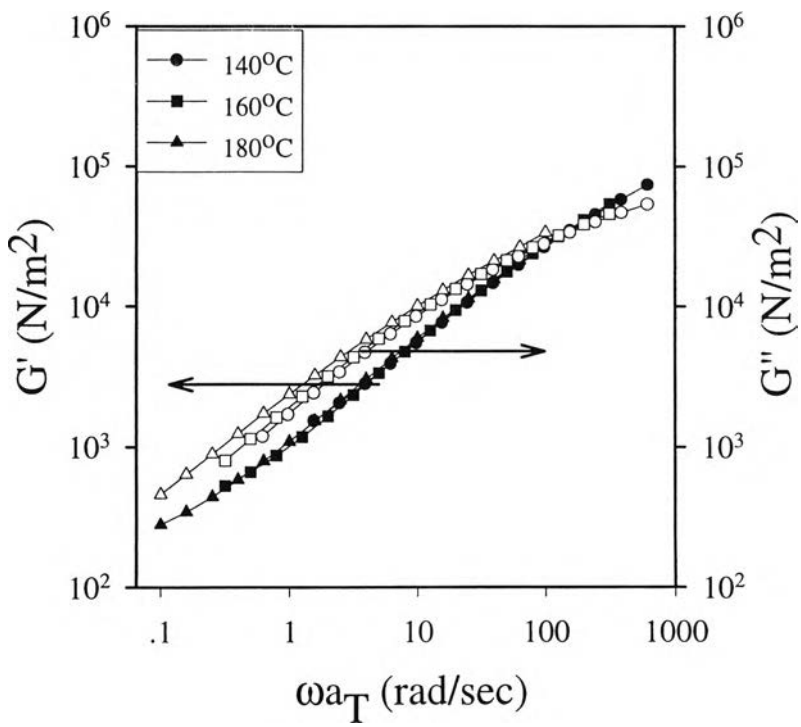

Figure 4.40 Storage and loss modulus master curve of 70/30/5 LLDPE/NR/MA blend at the reference temperature 180°C.

Figure 4.39 shows the G' and G" master curve of uncompatibilized blend. We can see that the two sets of G' and G" data determined at 160 and 180°C superpose very well in the full range of frequencies. But the data measured at 140°C showed a quite different behavior with strong deviation at high frequency. This deviation is most likely due to morphology modification at a higher stress or straining rate. It is obvious that for uncompatibilized blend, the assumption of a_T being independent of time (or frequency) is unjustified. Consequently, the LLDPE/NR blends are found to be thermorheologically complex unable to follow the time-temperature master curves. The storage and loss modulus master curves of compatibilized blend are shown in Figure 4.40. It is seen that there is good superposition of the G' data onto a single curve. Using the same shift factors a_T and reference temperature as used in G', superposition of G" was attempted. There is a clear breakdown of time-temperature superposition, particularly at low frequencies due to the slightly morphology difference as seen in the previous section.